Boise State University

ScholarWorks

Geosciences Faculty Publications and Presentations

Department of Geosciences

9-2022

Diverse Magmatic Evolutionary Trends of the Northern Andes Unraveled by Paleocene to Early Eocene Detrital Zircon Geochemistry

James L. Crowley
Boise State University

Publication Information

Jaramillo, Juan S.; Zapata, Sebastian; Carvalho, Monica; Cardona, Agustin; Jaramillo, Carlos; Crowley, James L.; . . . and Caballero-Rodriguez, Dayenari. (2022). "Diverse Magmatic Evolutionary Trends of the Northern Andes Unraveled by Paleocene to Early Eocene Detrital Zircon Geochemistry". *Geochemistry, Geophysics, Geosystems, 23*(9), e2021GC010113. https://doi.org/10.1029/2021GC010113

This document was originally published in *Geochemistry, Geophysics, Geosystems* by Wiley on behalf of the American Geophysical Union. Copyright restrictions may apply. doi: https://doi.org/10.1029/2021GC010113

Check for updates

Geochemistry, Geophysics, Geosystems®

AGU ADVANCING EARTH AND SPACE SCIENCE

RESEARCH ARTICLE
10.1029/2021GC010113

Special Section:
A fresh look at the Caribbean plate geosystems

Diverse Magmatic Evolutionary Trends of the Northern Andes Unraveled by Paleocene to Early Eocene Detrital Zircon Geochemistry

Juan S. Jaramillo[1,2], Sebastian Zapata[1,3,4], Monica Carvalho[1,5], Agustin Cardona[2], Carlos Jaramillo[1], James L. Crowley[6], Germán Bayona[7], and Dayenari Caballero-Rodriguez[1]

[1]Smithsonian Tropical Research Institute, Ancón, Panamá, [2]Universidad Nacional de Colombia, Medellín, Colimbia, [3]Facultad de Ciencias Naturales, Universidad del Rosario, Bogotá, Colombia, [4]Department of Geology and Geophysics, Missouri University of Science and Technology, Rolla, MO, USA, [5]Museum of Paleontology and Department of Earth and Environmental Sciences, University of Michigan, Ann Arbor, MI, USA, [6]Department of Geosciences, Boise State University, Boise, ID, USA, [7]Corporación geológica ARES, Bogotá, Colombia

Abstract The Paleocene-early Eocene continental magmatic arc (PECMA) in the Northern Andes is an example of arc magmatism following a major collisional event. This arc formed after the arc-continent collision between the Caribbean Plate and the South American continental margin at ca. 72 Ma. We used detrital zircon LA-ICP-MS and CA-ID-TIMS geochronology and geochemistry to complement the limited plutonic record of the PECMA and better characterize the PECMA's magmatic evolution. Zircon geochronology and their respective trace element geochemistry were analyzed from Paleocene-early Eocene strata of the Bogotá Formation in the foreland region. Our results show that after the collision of the Caribbean Plate, the magmas in the PECMA differentiated under a thick continental crust with limited subduction input at ca. 66 Ma. By 62–50 Ma, scattered patterns of Hf, U, U/Yb, and Yb/Gd ratios in detrital zircons suggest the existence of contrasting magmatic inputs attributed to different depths of crustal fractionation, varied temperatures of crystallization, and significant mantle and subduction inputs. These diverse magmatic patterns reflect the evolution of the continental crust. We proposed that oblique convergence and strike-slip tectonics favored contrasting crustal architectures along the continental margin while local lithosphere dripping from a previously thickened crust promoted the formation of hot magmas under a thick continental crust.

Key Points:

- Detrital zircon geochemistry was used to better refine the post-collisional Paleocene to Eocene tectono-magmatic evolution of the Northern Andes
- The Paleocene-early Eocene detrital zircons crystallized in contrasting magmatic conditions and under varying crustal thicknesses
- Strike-slip tectonics, crustal dripping, and a previously thickened continental crust can explain the observed diverse magmatic trends

Supporting Information:

Supporting Information may be found in the online version of this article.

Correspondence to:

J. S. Jaramillo,
jusjaramillori@unal.edu.co

Citation:

Jaramillo, J. S., Zapata, S., Carvalho, M., Cardona, A., Jaramillo, C., Crowley, J. L., et al. (2022). Diverse magmatic evolutionary trends of the Northern Andes unraveled by Paleocene to early Eocene detrital zircon geochemistry. *Geochemistry, Geophysics, Geosystems*, *23*, e2021GC010113. https://doi.org/10.1029/2021GC010113

Received 23 AUG 2021
Accepted 16 AUG 2022

© 2022. The Authors.
This is an open access article under the terms of the Creative Commons Attribution-NonCommercial-NoDerivs License, which permits use and distribution in any medium, provided the original work is properly cited, the use is non-commercial and no modifications or adaptations are made.

1. Introduction

The spatial distribution and composition of magmatic arcs are controlled by interactions between the mantle and the upper and lower plates, led by tectonic processes that typically last over one to tens of millions of years (Ducea et al., 2015; Gerya & Meilick, 2011; Paterson & Ducea, 2015; Syracuse & Abers, 2006). The plutonic and volcanic products that result from these interactions reflect different stages of the magmatic evolution: whereas plutonic rocks represent a more homogenized final record of a magmatic event, volcanic rocks are a snapshot of the magmatic settings at the time of the eruption (e.g., Glazner et al., 2015; Zimmerer & McIntosh, 2012).

Andean-type orogens are characterized by coeval magmatism, exhumation, and surface uplift (Bayona et al., 2021; Horton, 2018; Horton et al., 2010, 2015). These concurrent events often result in the erosion of the uppermost segment of the volcanic arcs (volcanic and shallow plutonic rocks) and in the exposure of deeper plutons (e.g., Barth et al., 2013; Yang et al., 2012). The exhumation and erosion of the initial magmatic products often biases the record of past volcanic arcs (Gaschnig et al., 2017).

Despite this bias, some of the volcanic arc's older record can be preserved in adjacent basins and their study can provide additional insights into the magmatic system (Barth et al., 2013; Malusà et al., 2011; McKenzie et al., 2018; Schwartz et al., 2021; Yang et al., 2012). Magmatic zircons provide the isotopic and chemical composition of the system at the time of their crystallization (Cavosie et al., 2005; Grimes et al., 2015; Vervoort et al., 2004). Because these minerals are resistant to low grade metamorphism, weathering, and sedimentary processes, they can retain their geochemical signatures after transport and burial (Morton & Hallsworth, 2007; Rubatto, 2017). The record of detrital zircons found in sedimentary basins adjacent to magmatic arcs can therefore provide evidence of their isotopic and chemical signatures (Barth et al., 2013; Cavosie et al., 2005, 2006; McKenzie et al., 2018; Yang et al., 2012).

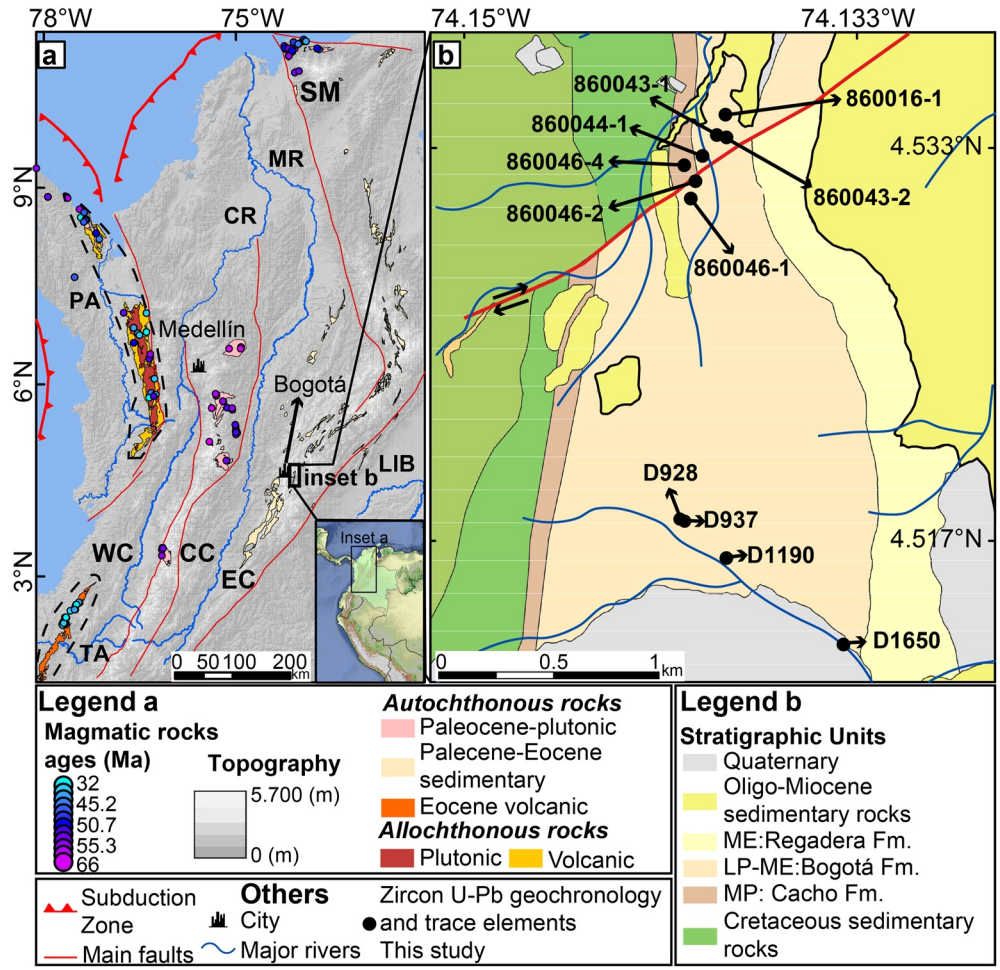

Figure 1. (a) Regional map showing the Paleocene-Eocene volcanic, plutonic, and sedimentary units in the Colombian Andes; circles denote the available radiometric ages. (b) Detailed geological map of the study region modified from Acosta and Ulloa (1998). WC: Western Cordillera, CC: Central Cordillera, EC: Eastern Cordillera, SM: Santa Marta Massif, LlB: Llanos Basin, PA: Allochthonous Panama Arc, CR: Cauca River, MR: Magdalena River, TA: Timbiquí Arc.

In the Northern Andes, the Late Cretaceous collision between the Caribbean and the South American Plates led to intense deformation, crustal thickening, and topographic growth along the continental margin (Bayona et al., 2012; Jaramillo et al., 2017; Kennan & Pindell, 2009; León et al., 2021; Pindell & Kennan, 2009; Villagómez & Spikings, 2013; Zapata et al., 2021). During the Paleocene and early Eocene, subduction of the Caribbean Plate formed a post-collisional magmatic arc along the South American continental margin (Paleocene–early Eocene continental magmatic arc, PECMA). The plutonic remnants of this arc are partially preserved and exposed in the Central Cordillera and Caribbean regions of Colombia, but the volcanic components are either not exposed nor preserved (Figure 1a) (Bayona et al., 2010, 2012; Bustamante et al., 2017; Cardona et al., 2011, 2018; Duque-Trujillo, Orozco-Esquivel et al., 2019; Leal-Mejía et al., 2019; Ordoñez et al., 2001). Based on this limited record, the subduction of the Caribbean Plate beneath a thick continental crust (Bayona et al., 2012; Bustamante et al., 2017) and slab break-off at ca. 58 Ma (Leal-Mejía, 2011; Leal-Mejía et al., 2019) have been proposed as the tectonic scenarios that controlled the post-collisional magmatic evolution. The absence of a more complete magmatic record, however, hinders the understanding of the evolution of the NW South American margin.

The PECMA was built on top of the basement (Permian-Triassic metamorphic rocks and Cretaceous igneous and sedimentary rocks) of the Central Cordillera and the Santa Marta Massif, which have had a positive high-relief since the Late Cretaceous. These high relief regions acted as a sediment source for adjacent basins including the foreland basins to the East (Bayona et al., 2012, 2021; Horton et al., 2015; Zapata et al., 2021). The middle Paleocene-early Eocene Bogotá Formation is a ca. 1.4 km-thick clastic sequence located in the axial zone of the

Eastern Cordillera, around 150 km east of the Central Cordillera (Figure 1a). Triassic, Jurassic, Cretaceous, and Paleocene-early Eocene populations of detrital zircons suggest that the basement of the Central Cordillera (basement of the PECMA) and the PECMA were the dominant source areas for the sediments of the Bogotá Formation (Bayona et al., 2010, 2012, 2021). Given that maximum depositional ages (MDA) of sandstones of the Bogotá Formation and Paleocene–early Eocene populations of detrital zircons become progressively younger toward the top of the sequence, it is likely that vulcanism of the PECMA was nearly coeval with sedimentation in this basin (Alberts et al., 2021; González et al., 2018; Rodríguez-Alonso et al., 2004). We used LA-ICP-MS and CA-ID-TIMS detrital zircon geochronological and geochemical constraints from the Bogotá Formation to improve our understanding of the PECMA. The integration of this detrital record with data from exposed plutonic rocks (Bustamante et al., 2017; Cardona et al., 2011, 2018; Duque-Trujillo, Orozco-Esquivel et al., 2019; Leal-Mejía et al., 2019) provides further insight into the dynamics of convergent margin tectonic settings, especially after the transition from collision to subduction (Brown & Ryan, 2011; Draut & Clift, 2001).

2. Cretaceous to Eocene Tectonic Evolution of the Northern Colombian Andes (6–12°N)

The basement of the Western Cordillera of Colombia is a remnant of the allochthonous Caribbean Plate–a thick oceanic plateau and intraoceanic arc accreted to the continental margin during the Late Cretaceous (ca. 72 Ma) (George et al., 2021; Jaramillo et al., 2017; Kennan & Pindell, 2009; Kerr et al., 1997; Pardo-Trujillo et al., 2020; Pindell & Kennan, 2009; Restrepo & Toussaint, 1988; Villagómez & Spikings, 2013). Various sources of evidence–thermo-kinematic models, stratigraphy, and crustal thickness estimates based on whole-rock geochemistry–suggest that the collision of this plate caused the deformation, uplift, and exhumation of the pre-Cretaceous basement that is currently exposed in the Central Cordillera (Bustamante et al., 2017; León et al., 2021; Zapata et al., 2021; Zapata-Villada et al., 2021).

The onset of subduction after the collision was responsible for the development of PECMA. U-Pb zircon ages from exposed plutons show that magmatism started at ca. 62 Ma and ceased at ca. 50 Ma. The age of this plutonic record has been interpreted as evidence of a hiatus between the collision (ca. 72 Ma) and the onset of subduction (Bayona et al., 2012; Bustamante et al., 2017; Cardona et al., 2018; Duque-Trujillo, Bustamante, et al., 2019; Leal-Mejía et al., 2019). Magmatism has also been interpreted as a product of asthenospheric upwelling driven by a post-collisional slab break-off (Leal-Mejía, 2011; Leal-Mejía et al., 2019), yet this interpretation assumes that the collision of the Caribbean Plate and the NW South American continental margin occurred during the Eocene. An Eocene collision does not agree with time constraints based on the intrusion of undeformed plutonic rocks that show evidence of an earlier, Late Cretaceous collision (Bustamante et al., 2017; Duque-Trujillo, Bustamante, et al., 2019; Jaramillo et al., 2017; Villagómez & Spikings, 2013; Zapata-Villada et al., 2021). During the Oligocene, the northern segment of the PECMA was fragmented and became displaced, resulting in the formation of the Santa Marta Massif and Guajira ranges (Kennan & Pindell, 2009; Montes et al., 2010, 2019; Parra et al., 2020; Pindell & Kennan, 2009; Weber et al., 2010).

This Late Cretaceous-Paleocene collisional orogenic phase resulted in the development of high topography that became the source area of adjacent syn-orogenic basins to the east (Bayona et al., 2021; León et al., 2021; Pardo-Trujillo et al., 2020; Zapata et al., 2021). The syn-orogenic middle Paleocene-early Eocene continental succession of the Bogotá Formation (61-50 Ma) corresponds to a fluvial system that accumulated under high subsidence rates in a basin adjacent to the PECMA (Figure 1a) (Bayona et al., 2012, 2021). Fluvial sediments were mainly sourced from the paleo-Central Cordillera and the PECMA in addition to several intrabasinal uplifts (Montes et al., 2012) and smaller volcanic sources within the basin (Bayona et al., 2012, 2021; Caballero et al., 2020).

In addition to the PECMA, two other Paleocene-Eocene magmatic arcs are currently exposed in the Northern Andes (Figure 1a). These comprise (a) the Timbiqui continental volcanic arc (~55-35 Ma) that intruded the oceanic basement of the Western Cordillera south of 3°N (Barbosa-Espitia et al., 2019; Cardona et al., 2018), and (b) the allochthonous oceanic Panama-Chocó arc exposed along the western flank of the Western Cordillera and the Pacific coast north of 4°N (Barbosa-Espitia et al., 2019; León et al., 2018; Montes et al., 2015; Villagómez et al., 2011; Zapata-García & Rodríguez-García, 2020). These arcs are, however, unlikely sources of sediments for the Bogotá Formation given that the Timbiqui arc is significantly younger, and the Panama arc formed in a

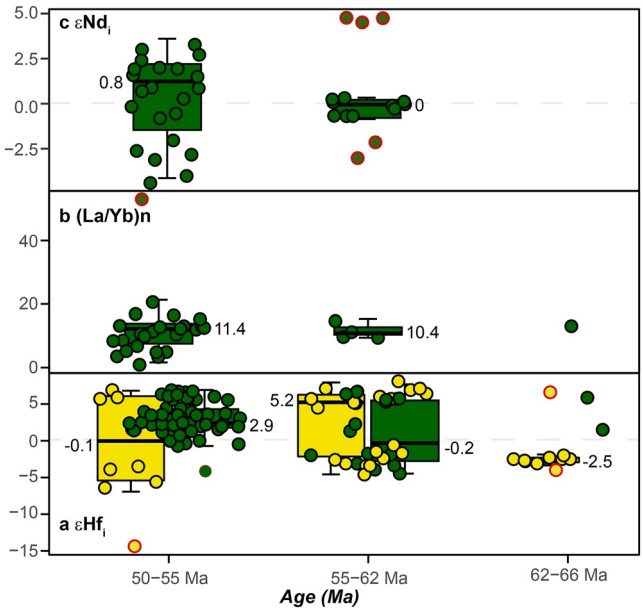

Figure 2. Compiled whole-rock analyses from the Paleocene-early Eocene continental magmatic arc (PECMA) plutonic rocks (Bustamante et al., 2017; Cardona et al., 2011, 2018; Leal-Mejía et al., 2019; Ordoñez et al., 2001; Rueda-Gutiérrez, 2019). (a) Age (Ma) versus Zircon εHf values from plutonic (green circles) and detrital zircons (yellow circles). (b) Age (Ma) versus La/Yb normalized to the chondrite composition (McDonough & Sun, 1995). (c) Age (Ma) versus εNd whole-rock geochemical data obtained from in situ plutons, the boxplots show the error bars, and thick lines correspond to the mean values after removing outliers (red borders).

distal position, SW of the continental margin, and collided with the continental margin in the Middle Miocene (León et al., 2018; Montes et al., 2015).

3. Previous Paleocene-Eocene Whole-Rock and Zircon Geochemical and Isotopic Data

The magmatic record of the PECMA in the Colombian Andes is restricted to plutonic rocks exposed in the Central Cordillera and Santa Marta Massif. These rocks have been interpreted as part of an active magmatic arc characterized by U-Pb zircon ages between 62 and 50 Ma with calc-alkaline and adakite-like geochemical signatures (Bustamante et al., 2017; Cardona et al., 2011, 2018; Leal-Mejía et al., 2019) (Bayona et al., 2012; Bustamante et al., 2017; Cardona et al., 2018; Duque-Trujillo, Orozco-Esquivel et al., 2019; Leal-Mejía et al., 2019). Currently, evidence of PECMA magmatism earlier than 60 Ma is restricted to small plutons in the Santa Marta Region (Cardona et al., 2011; Duque-Trujillo, Orozco-Esquivel et al., 2019) and antecrysts in younger, Late Paleocene plutons (Bustamante et al., 2017). These antecrysts have $\varepsilon Hf_{(i)}$ values between +1.5 and +5.9 (Figure 2a), which are characteristic of zircons formed in magmas that derived from the mantle (Iizuka et al., 2017) and were modified by assimilation of an older continental crust (Bustamante et al., 2017; Cardona et al., 2018).

Plutons between 62 and 50 Ma show whole rock (La/Yb)n ratios between 3.3 and 19.7 (Figure 2b) that suggest crustal thickness values between 39 and 59 km (Bustamante et al., 2017; León et al., 2021). These also show whole-rock $\varepsilon Nd_{(i)}$ values between −3 and +4 while $\varepsilon Hf_{(i)}$ values range between −4.2 and +6.9 (Figures 2a and 2c) that indicate both mantle and crustal inputs (Bustamante et al., 2017; Cardona et al., 2011, 2018; Leal-Mejía et al., 2019; Ordoñez et al., 2001).

Zircons with ages between 66 and 62 Ma have $\varepsilon Hf_{(i)}$ values between −4.0 and −2.0 in addition to a single grain with an $\varepsilon Hf_{(i)}$ of +6.6; those with ages between 62 and 50 Ma have a higher variation in $\varepsilon Hf_{(i)}$ values and range between −14.4 and +8.1 (Figure 2a) (Bustamante et al., 2017). These isotopic data also suggest different amounts of mantle and crustal contributions throughout the magmatic evolution of the PECMA.

4. Methods

4.1. Field Observations and Sampling Strategy

Eight samples of fluvial sandstones and a reworked volcanic tuff were collected from two stratigraphic sections of the Bogotá Formation. These are separated less than 3 km apart and crop out in the Parque Industrial Mochuelo, Bogotá Colombia (Figure 1b). The sections comprise thick, mottled mudstone beds with paleosol development (argillisols and oxisols) (Morón et al., 2013), interbedded fine-grained to conglomeratic fluvial sandstones, volcaniclastic sandstones, and a reworked volcanic tuff. Figure 4 shows the relative stratigraphic position of the analyzed samples. All samples were collected as part of previous stratigraphic and paleontological studies carried out in an area with abundant leaf beds and vertebrates that record the Paleocene-early Eocene global warming events (e.g., Bayona et al., 2012; Jaramillo & Cárdenas, 2013; Moron et al., 2013). In this location, the Bogotá Formation is interpreted as a middle Paleocene-early Eocene meandering to a braided fluvial depositional system sourced from the west (Bayona et al., 2010, 2021). This unit is conformably overlying the middle Paleocene sandstones of the Cacho Formation, and it is unconformably overlain by middle to upper Eocene fluvial conglomeratic sandstones of the Regadera Formation (Bayona et al., 2010). Both the Cacho and Regadera formations lack evidence of syn-sedimentary magmatism.

4.2. Zircon U-Pb Geochronology

Zircon U-Pb geochronology and geochemistry have been widely used to reconstruct the evolution of magmatic rocks (Schaltegger et al., 2015). Given that sedimentary transport and diagenesis do not significantly modify

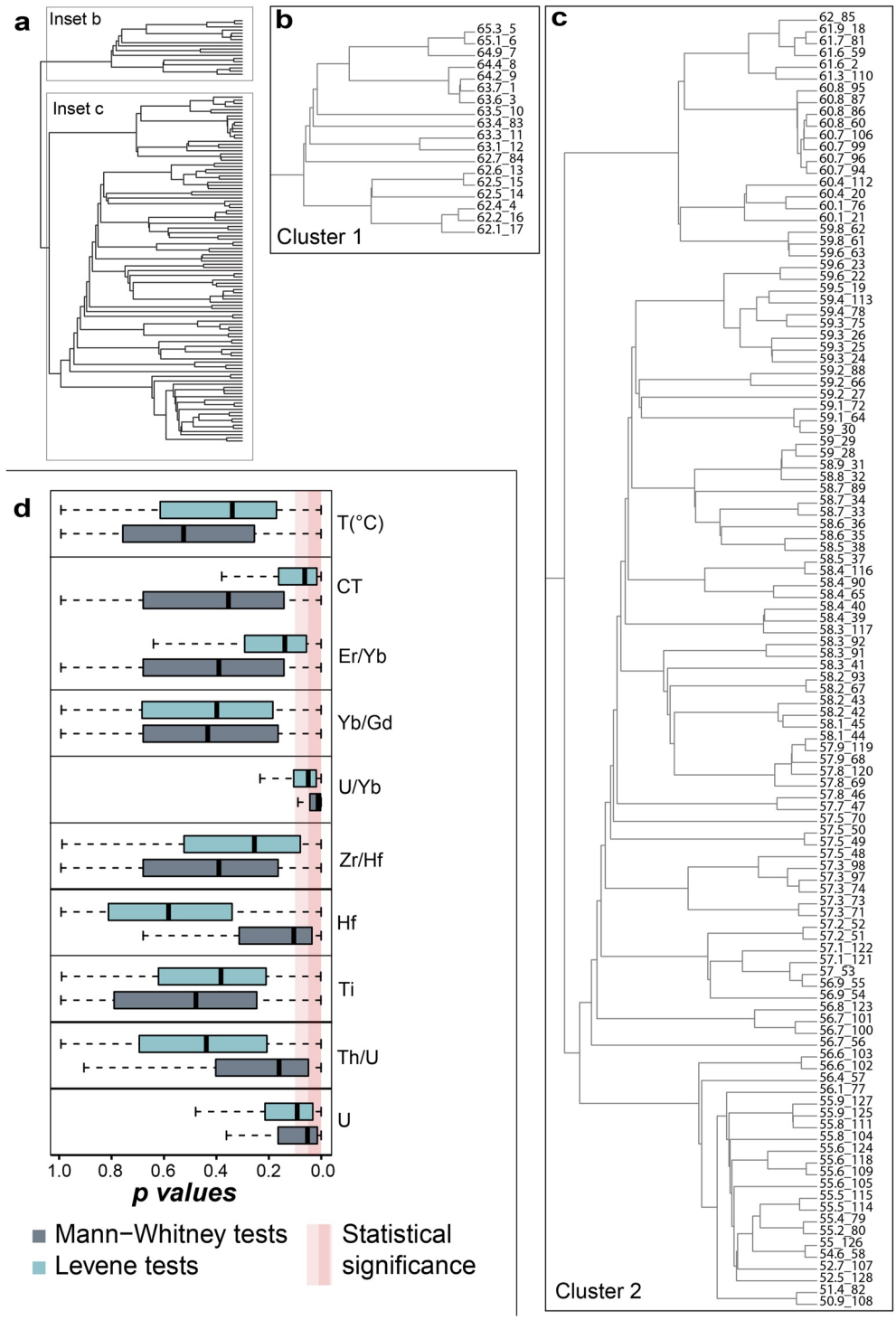

Figure 3. (a) Summary of the cluster analysis created using Euclidean distance and coniss agglomeration method on the geochemical composition of 126 Paleogene detrital zircons. Two main clusters are shown and detailed in (b, c) (b) Detail of Cluster 1, grouping older zircons (66.0 to 62.0 Ma). (c) Detail of Cluster 2, grouping younger zircons (62.0 to 50.9 Ma). (d) Distribution of *p*-values from Mann-Whitney and Levene tests used for comparing the mean values and variance of 10 geochemical parameters between older and younger zircons (Cluster 1 and 2, respectively). CT: Crustal thickness estimates based on Eu anomaly; T (°C): Magma temperature estimated from Ti values.

zircon geochemical composition, detrital grains can be used to constrain the ages and the composition of the magmatic sources (Gehrels, 2014; Horton et al., 2015).

Zircon U-Pb dating was obtained by Laser Ablation-Inductively Coupled Plasma-Mass Spectrometry (LA-ICP-MS) and Chemical Abrasion-Isotope Dilution-Thermal Ionization Mass Spectrometry (CA-ID-TIMS) in the isotope geology laboratory at Boise State University, Boise, Idaho, USA. Detailed analytical procedures for each technique are presented in Text S1 and Text S2 in Supporting Information S1 (Condon et al., 2015; Gerstenberger & Haase, 1997; Hiess et al., 2012; Jaffey et al., 1971; Kennedy et al., 2014; Krogh, 1973; Ludwing, 2003; Schmitz & Schoene, 2007; Sláma et al., 2008). LA-ICP-MS is often used to obtain large amounts of single-grain zircon dates with errors <5% (Gehrels et al., 2008; Schaltegger et al., 2015). In CA-ID-TIMS damaged regions within zircon crystals that may have lead loss are removed, resulting in highly accurate and precise dates (errors <0.1%) (Black et al., 2004; Crowley et al., 2007; Mattinson, 2005). Combining these two techniques is the most adequate method to identify detrital age populations and to obtain dates that can resolve high-resolution stratigraphic or magmatic problems (Cilliers et al., 2021; Herriott et al., 2019).

Zircons separated from the nine samples from the Bogotá Formation were analyzed with LA-ICP-MS to obtain U-Pb dates and trace element concentrations (Table S1, https://doi.org/10.6084/m9.figshare.19131857). Only sharply faceted, euhedral crystals were analyzed with the aim to increase the chances of collecting data from the young volcanic grains and avoid older crystals that could have undergone multiple sedimentation cycles (Cretaceous to Precambrian). This procedure may have created a bias in the zircon populations; however, this contribution focuses on the magmatic evolution of the Paleocene-Eocene magmatic arc and does not intend to answer a question of provenance. Various provenance analyses have already been previously carried out in the Bogotá Formation (Bayona et al., 2010, 2012, 2021).

The zircons that yielded the youngest LA-ICP-MS dates were further dated using CA-ID-TIMS. Twenty-nine zircon grains from three clastic samples (860046-2, D1190, and D1650) and one from a reworked tuff sample (D928) were analyzed using CA-ID-TIMS (Tables 1 and S2, https://doi.org/10.6084/m9.figshare.19131857). Sample locations are presented in Table 1 and Figure 1b. Figures 4 and S2 in Supporting Information S1 show the Kernel density estimates (KDEs), concordance plots, and MDA estimated using the radial plot method (Vermeesch, 2021). Each sample was plotted using Isoplot R (Vermeesch, 2018). We discuss and interpret zircon data from 128 grains (seven samples) with dates between 66 and 50 Ma. We only considered zircon grains that had ages with 2σ errors lower than 4 Ma.

4.3. Zircon Geochemistry and Estimates of Crustal Thickness

The relative concentration of trace elements in zircons is controlled by multiple magmatic processes. For instance, Hf, Th, and U can be directly associated with specific magma compositions and are therefore indicative of magma compositional differentiation and crustal assimilation (Claiborne et al., 2006; Kirkland et al., 2015). Yb and Y can be preferentially trapped in minerals crystallized at high pressures, which allows inferring crystallization depths (Barth et al., 2013), and Ti content is dependent upon magma temperatures (Ferry & Watson, 2007).

The crustal thickness was estimated following Tang et al. (2021). This approach is based on the Eu anomaly (Eu/Eu* ratio), which is sensitive to fractionation under varying pressure (Tang et al., 2021). Under high pressures, the preferential incorporation of Fe^{+2} into garnet enhances the oxidation of multivalent trace elements such as Eu (Tang et al., 2018, 2019). The oxidation of Eu increases the availability of Eu^{+3} concerning Eu^{+2} and facilitates the incorporation of Eu in the zircon lattice. As a consequence, zircons crystallized under high pressure and crustal thickness exhibit lower Eu anomalies evidenced in higher Eu/Eu* ratios. Conversely, shallow magma fractionation will result in higher Eu anomalies and low Eu/Eu* ratios (Tang et al., 2021). Crustal thickness values derived from zircon geochemistry are nonetheless approximations and need to be interpreted carefully, as Eu/Eu* ratios may be affected by different magmatic processes such as assimilation of mature basements, co-crystallization of plagioclase, and zircon at shallow depths, and variations in the redox state of the melts (Holder et al., 2020; Tang et al., 2021).

We used cathodoluminescence and reflected images to avoid ablating close to zircon inclusions. Additionally, the geochemical signatures of zircons with Th/U > 0.1, $P > 500$, and Lan > 30 were discarded to prevent potential contamination induced by inclusions (apatite, monazite, rutile, etc.), metamictization, and metamorphism.

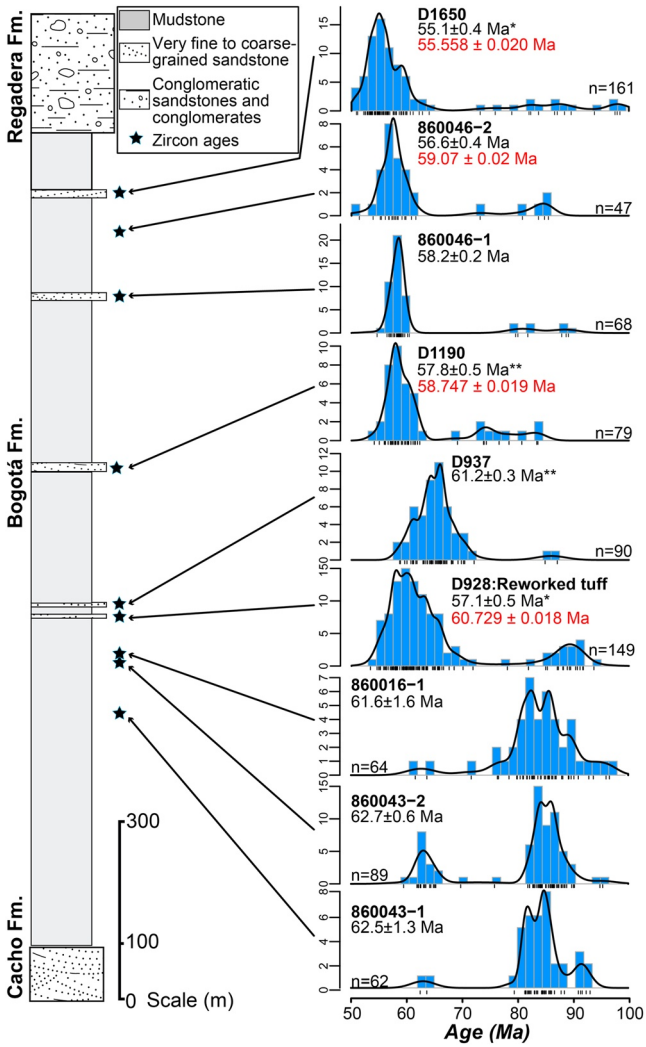

Figure 4. Generalized stratigraphic section of the Bogotá Formation (modified from Bayona et al., 2012). Blue stars denote the samples with zircon geochronological and geochemical data and the rectangles are samples without zircon REE data, compiled from Bayona et al. (2012). KDE distributions are presented for each sample showing only the Paleocene-Eocene geochronological data. The red number corresponds to the younger CA-ID-TIMS age while the black number indicates maximum depositional ages calculated with the unmixed radial plot method (Vermeesch, 2021).

4.4. Statistical Analysis of Trace Element Composition

A cluster analysis using Euclidean distance and coniss agglomeration method (package "rioja," Juggins, 2020) was performed in zircons with ages between 66 and 50 Ma to identify general patterns in zircon composition over time. This analysis used a distance matrix based on U, Hf, Ti contents, Th/U, Zr/Hf, U/Yb, Yb/Gd, and Er/Yb ratios and estimates of temperature and crustal thickness. We followed the silhouette width criterion to evaluate the optimal number of clusters (Kaoungku et al., 2018). Two clusters (Figure S3 in Supporting Information S1) were identified based on age and similarities in geochemical composition (Figures 3a–3c), grouping zircons dated between 66.0 and 62.0 Ma and between 62.0 and 55.0 Ma. We compared the geochemical composition of zircons dated between 66.0 and 62.0 Ma to those between 62.0 and 55.0 Ma (Figure 3d). Because the sample size was not constant across these two age intervals, we subsampled each age group (n = 10 zircons) to test for differences in mean values and variance of U, Hf, Ti contents, Th/U, Zr/Hf, U/Yb, Yb/Gd, and Er/Yb ratios, and estimates of temperature and crustal thickness. For each subsample, we applied a Mann-Whitney U test (Mann & Whitney, 1947) to assess differences in the mean, and Levene tests (Levene, 1960) to contrast the variance of these across age groups. The subsampling and statistical tests were iterated 1,000 times, and the distribution of p-values resulting from the Levene or Mann-Whitney tests are presented in Figure 3d and Table S3, https://doi.org/10.6084/m9.figshare.19131857. We consider differences in the chemical composition of zircons when the resulting p-value distribution is noticeably skewed toward zero, with the first quartile (LVQ1 and MWQ1 for Levene and Mann-Whitney tests, respectively) below 0.05 and median value close to 0.1. This statistical approach allows the identification of significant differences in the geochemical composition of zircon grains before and after 62 Ma.

5. Results

5.1. LA-ICP-MS and CA-ID-TIMS Geochronology

We analyzed 489 zircons that measure 60–390 μm long and have a length: width aspect ratios of 2:1–4:1 (Figure 5a). Under cathodoluminescence, the predominant zircon population exhibits oscillatory zoning (Figure 5a) characteristic of magmatic growth (Corfu et al., 2003). Some of these zircons show sector zoning which may be related to rapid changes in the growth conditions (e.g., temperature and growth rates) during crystal formation (B. A. Paterson & Stephens, 1992). Zircons with homogeneous cores and complex rims were interpreted as older xenocrysts with younger overgrowth (Miller et al., 2003).

LA-ICP-MS dates included Triassic (~238 Ma; n = 26), Jurassic (~160 Ma; n = 58), Late Cretaceous (~84 Ma, n = 197), and Paleocene (~59 Ma; n = 156) populations (Figure 5b), which despite the bias induced by the selection of sharply faceted grains are similar to the zircon age distributions presented in previous provenance studies (Bayona et al., 2012; Bustamante et al., 2017). Paleocene to early Eocene zircons range between 66.0 and 50.9 Ma and have a large population with dates ca. 57.7 Ma and a secondary population with dates ca. 62.8 Ma (Figure 5b).

Detrital zircon populations of Paleocene–Eocene age become progressively younger toward the top of the Bogotá Formation, suggesting that volcanism was contemporary with sediment deposition (Figure 4) (Alberts et al., 2021; González et al., 2018). The basal segment of the Bogotá Formation is characterized by zircon dates between 65.3 and 59.5 Ma (18 zircons) with MDA between 62.5 and 61.6 Ma (Figure 4). Samples from the upper stratigraphic segment show zircon dates between 66.0 and 50.9 Ma with MDA between 61.2 and

Table 1
Location and Maximum Depositional Ages Obtained From LA-ICP-MS and CA-ID-TIMS From the Nine Samples Analyzed

Sample	Lat	Long	Maximum depositional LA-ICP-MS age	Youngest CA-TIMS age
860016–1	4.53454	−74.13919	61.6 ± 1.6	
860043–1	4.53367	−74.13951	62.5 ± 1.3	
860043–2	4.53357	−74.13910	62.7 ± 0.6	
860046–1	4.53098	−74.14059	58.2 ± 0.2	
860046–2	4.53173	−74.14040	56.6 ± 0.4	59.07 ± 0.02
D928	4.53700	−74.16300	57.1 ± 0.5	60.68 ± 0.04
D937	4.53700	−74.16300	61.2 ± 0.3**	
D1190	4.53700	−74.16300	57.8 ± 0.5**	58.72 ± 0.04
D1650	4.53700	−74.16300	55.1 ± 0.4*	55.53 ± 0.04

55.1 Ma. Zircon grains with dates between 55.0 and 50.9 Ma are restricted to a few zircons at the top of the stratigraphic section (Figure 4), suggesting an early Eocene age for the uppermost beds of the Bogotá Formation (Bayona et al., 2012, 2021). The dates of detrital zircons from the Bogotá Formation obtained using LA-ICP-MS are overall older than the LA-ICP-MS dates from PECMA plutonic rocks (t-value = −16.526, degrees of freedom = 567.67, p-value < 2.2e−16) (Bustamante et al., 2017; Cardona et al., 2011, 2018; Leal-Mejía et al., 2019; Ordoñez et al., 2001; Rueda-Gutiérrez, 2019). Whereas detrital grains have a mean age of 59.4 Ma, plutonic zircons have a mean age of 55.7 Ma (Figure 6a). Therefore, our data represent older stages of the magmatic evolution that are not preserved in the plutonic record of the cordillera.

Detrital zircon grains (6–8 per sample) analyzed under CA-ID-TIMS yielded MDA between 55.53 ± 0.04 Ma and 60.68 ± 0.04 Ma (Table 1). Overall, dates obtained using CA-ID-TIMS are 0.4–3.6 Ma older than those obtained using LA-ICP-MS. These discrepancies may be related to lead loss or radiation damage which are not detected by LA-ICP-MS (Herriott et al., 2019).

5.2. Trace Element Composition of Detrital Zircons From the Bogotá Formation

A cluster analysis based on the age and geochemical composition of 128 Paleocene-early Eocene detrital zircon grains is shown in Figures 3a–3c. The silhouette width criterion recognizes two distinct clusters (Figure S3 in Supporting Information S1) that group zircons between 66.0 and 62.0 Ma (n = 18) and those between 62 and 50 Ma (n = 110). These results suggest changes in magma composition and crystallization conditions over time (before and after 62.0 Ma). Trace elements in older zircon grains (66.0–62.1 Ma) are less variable than in younger grains (62–55 Ma) (Figures 6 and 7). Even though a larger number of younger zircon grains can account for a higher heterogeneity, U, Hf, U/Yb, and crustal thickness values show statistically distinctive trends before and after 62 Ma despite differences in the numbers of zircons (see Section 4.4 and Figure 3d).

The content of U across the 128 Paleocene-early Eocene detrital zircons analyzed ranges between 60 and 2,200 ppm, and Th/U ratios range between 0.1 and 1.4. U content (mean values and variance) differs significantly between

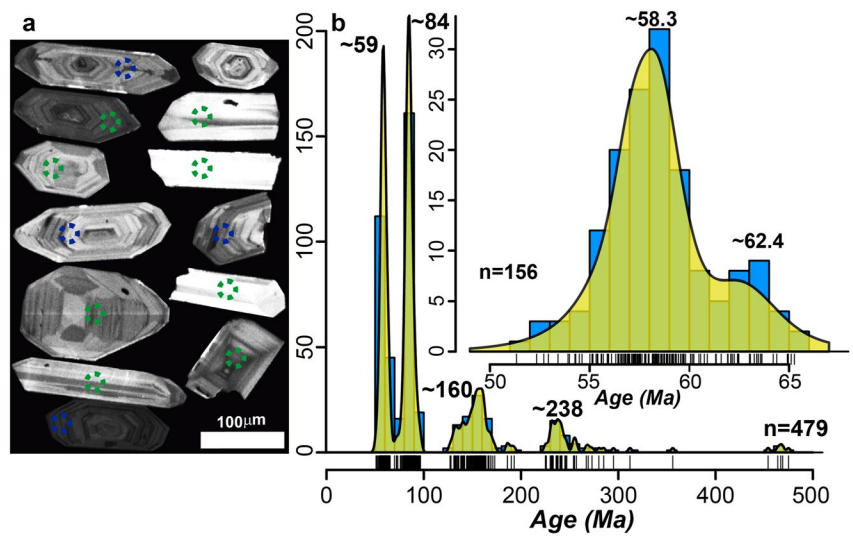

Figure 5. (a) Cathodoluminescence of representative Paleocene-Eocene detrital zircons. Blue circles indicate grains with CA-ID-TIMS ages and geochemical data obtained using LA-ICP MS. Green circles indicate grains with age and geochemical data obtained using LA-ICP-MS. Circles are 25 µm wide and indicate the position of the LA-ICP-MS laser spot. (b) Age distribution (blue) and kernel density estimation (yellow) of 479 detrital zircons. The inset contains age distribution for 156 zircons dated between 66 and 50 Ma. The black bars on the x-axis of KDE represent individual ages. Sample data are presented in Table S1, https://doi.org/10.6084/m9.figshare.19131857.

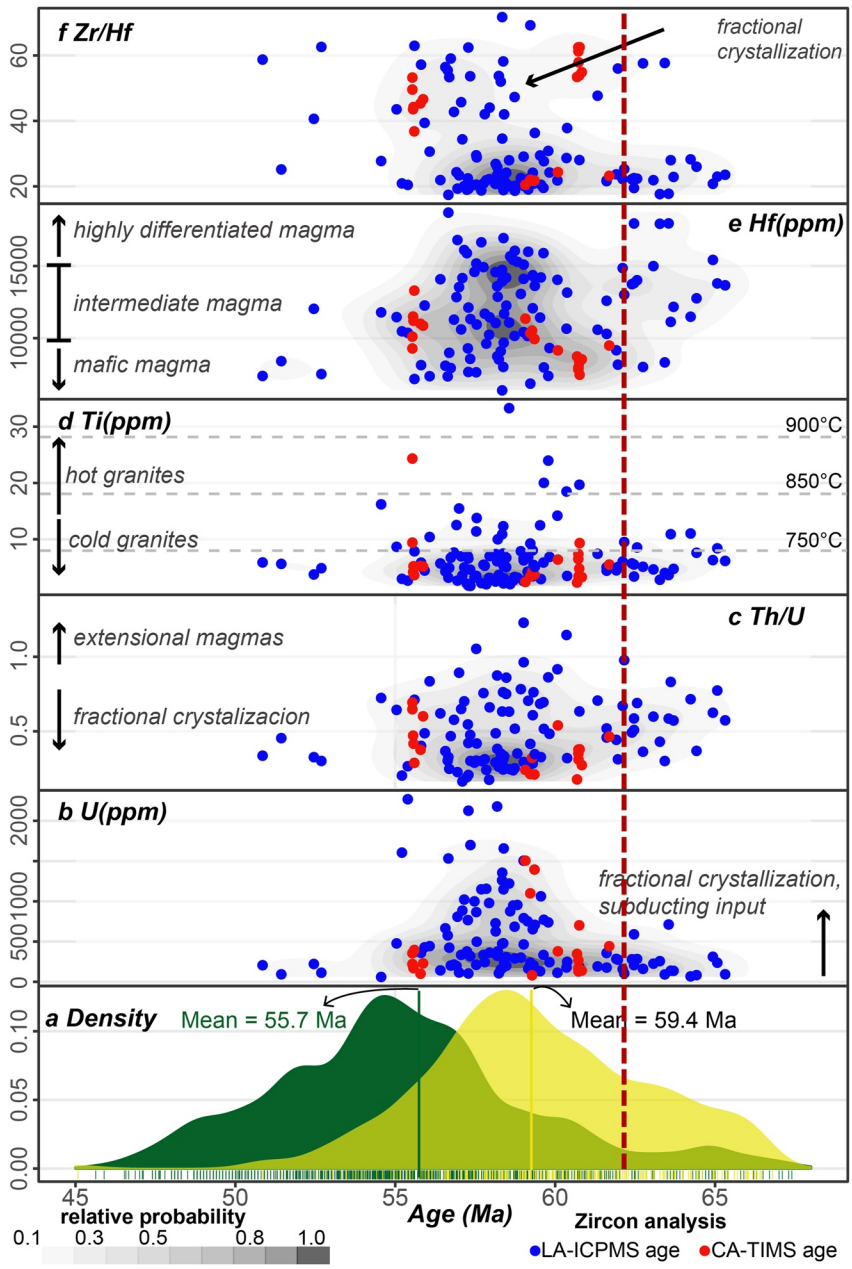

Figure 6. (a) Normalized probability density plot (PDP) of Paleocene-early Eocene continental magmatic arc (PECMA) zircon dates from the Central Cordillera (green shadow) (Bayona et al., 2012; Bustamante et al., 2017; Cardona et al., 2011, 2018; Duque-Trujillo et al., 2019; Rueda-Gutiérrez, 2019) and detrital zircon dates from the Bogotá Formation (yellow shadow) (Bayona et al., 2012; this work). (b) Age (Ma) versus U (ppm). (c) Age (Ma) versus Th/U. (d) Age (Ma) versus Ti (ppm) and the inferred saturation temperatures (Ferry & Watson, 2007). (e) Age (Ma) versus Hf (ppm). (f) Age (Ma) versus Zr/Hf. The dashed red box indicates the time interval between 62 and 55 Ma. Annotations are from Belousova et al. (2002); Claiborne et al. (2006, 2010); Kirkland et al. (2015); McKay et al. (2018); Yang et al. (2012).

the younger and older detrital zircon populations (LVQ1 = 0.03 and MWQ1 = 0.01; Figure 3d and Table S3, http://doi.org/10.6084/m9.figshare.19131857) even though no significant differences in Th/U ratios are observed (LVQ1 = 0.21 and MWQ1 = 0.05; Figure 3d; Table S3, http://doi.org/10.6084/m9.figshare.19131857). Ti values range between 1.7 and 33.2 ppm and do not show significant differences across both age groups (LVQ1 = 0.21 and MWQ1 = 0.25; Figure 3d). These Ti values correspond to zircon saturation temperatures between 937°C and 641°C. Hf content varies between 6,000 and 18,000 ppm and Zr/Hf ratios range between 17 and 71.7. Hf content in younger zircons differs from that in older zircons (MWQ1 = 0.04 and LVQ1 = 0.34), whereas Zr/Hf

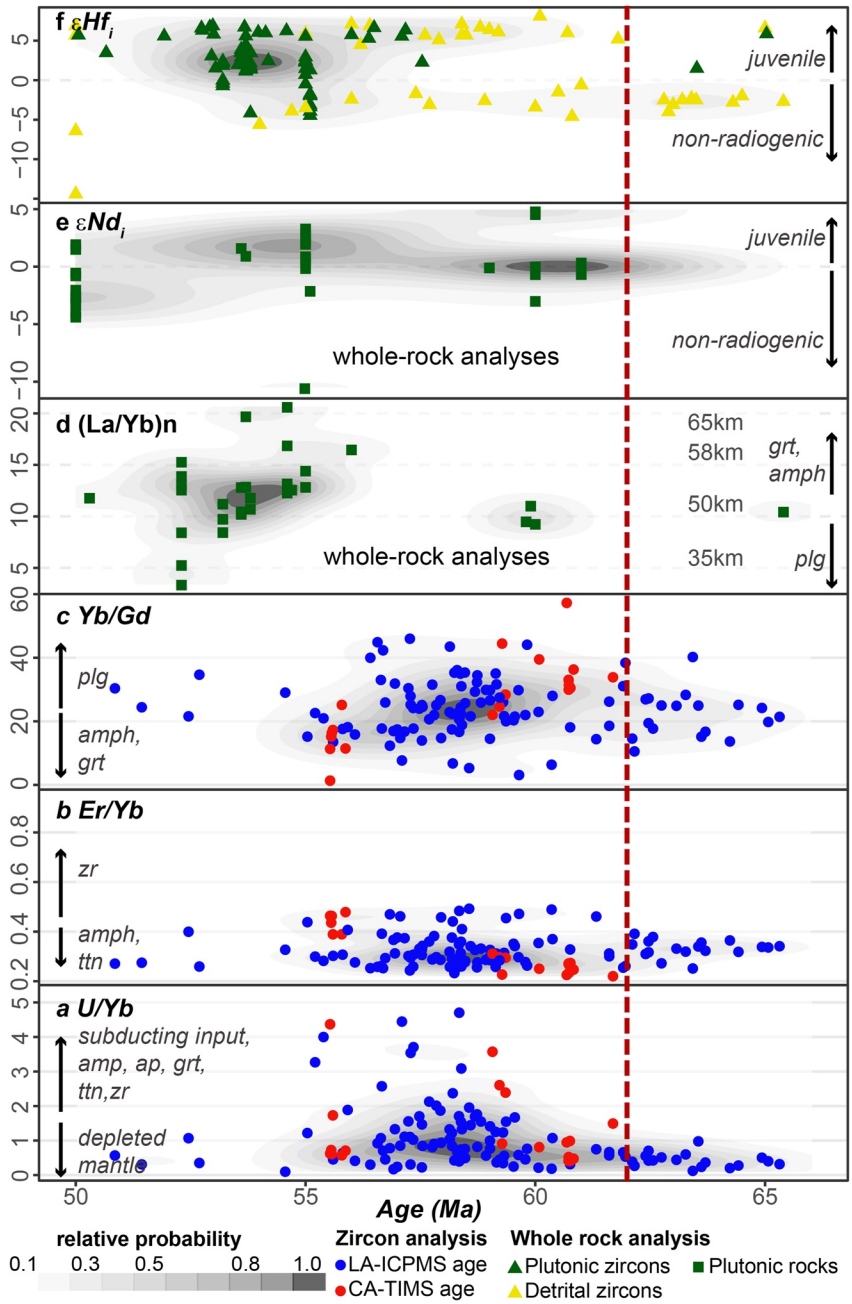

Figure 7. Whole-rock and detrital zircon geochemistry in relation to zircon age. (a) Age (Ma) versus U/Yb ratios. (b) Age (Ma) versus Er/Yb ratios. (c) Age (Ma) versus Yb/Gd ratios. (d) Age (Ma) versus Whole-rock geochemistry (La/Yb). (e) Age (Ma) versus Whole-rock Nd radiogenic isotope signatures. (f) Age (Ma) versus Hafnium isotopic signature in zircons from the Paleocene-early Eocene continental magmatic arc (PECMA) and detrital zircons from Bogotá Formation. Whole rock geochemical and isotopic data are from (Bustamante et al., 2017; Cardona et al., 2011; Duque-Trujillo et al., 2019; Leal-Mejía, 2011; Villagómez et al., 2011). Annotations are from Barth et al. (2013); Grimes et al. (2015); Profeta et al. (2015); and Sundell et al. (2021).

ratios show no significant differences in mean values or variance (LVQ1 = 0.08 and MWQ1 = 0.17; Figure 3d). U/Yb ratios vary between 0.1 and 5.3 and show differences in mean values and variances measured in younger and older zircons (LVQ1 = 0.02 and MWQ1 = 0.00; Figure 3d). Zircons older than 62 Ma have low U/Yb ratios (0.2–1.0), whereas the ratios measured in grains younger than 62 Ma are more widespread and range up to 5 (Figure 7a). Er/Yb ratios range between 0.2 and 0.9 with the highest values observed among the younger

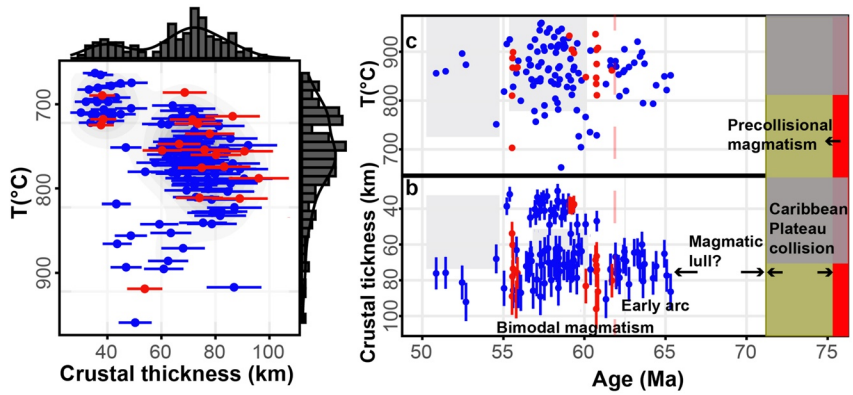

Figure 8. (a) Crustal thickness (km) versus Temperature (°C) with marginal histograms showing the bimodal behavior of the data. (b, c) Magmatic history of NW South America during the 75-50 Ma interval. (b) Age (Ma) versus Crustal thickness calculated using the methods presented by Tang et al. (2021), (c) Age versus Zircon Ti saturation temperature. Complete legend is presented in Figure 6. The magmatic lull between 72 and 66 Ma, the Caribbean Plate collision, and the pre-collisional magmatism are indicated with black arrows. Gray squares correspond to changes in temperatures and crustal thickness from published whole-rock geochemical data (Bustamante et al., 2017; Cardona et al., 2011; Duque-Trujillo et al., 2019; Leal-Mejia et al., 2019; Rueda-Gutiérrez, 2019).

grains (62 to 50 Ma), even though no significant differences between groups were found (MWQ1 = 0.14 and LVQ1 = 0.06; Figure 3d). Yb/Gd ratios range between 1.3 and 60 and show no differences in younger and older zircons (MWQ1 = 0.17 and LVQ1 = 0.19; Figure 3d). Estimates of crustal thickness based on Eu anomalies (Eu/Eu*) fall between 30.2 and 96 km. These estimates show a bimodal distribution with mean values of 41 ± 6 and 73 ± 9 km (Figures 8a and 8b). The smaller values of crustal thickness are only retrieved from younger zircons (62 to 50 Ma), and therefore the variance of estimated crustal thickness differs significantly between younger and older zircons (LVQ1 = 0.02). No significant difference was observed for mean values of the crustal thickness (MWQ1 = 0.14).

The composition of trace elements in detrital zircons dating between 95 and 73 Ma (n = 196) differs from that of PECMA-derived zircons. Cretaceous zircons are characterized by lower U content (<1,000 ppm) and U/Yb ratios (<1), a narrow range of Zr/Hf ratios (15–30), and smaller crustal thickness values (mean of 44.6 ± 8.1 km) when compared with the Paleogene zircons (Detailed results are presented in Figure S4 in Supporting Information S1).

6. Discussion

The deformation and exhumation phases that characterized the Late Cretaceous to Cenozoic tectonic evolution of the Northern Andes eroded the volcanic cover and shallow plutonic rocks on top of the PECMA (Bayona et al., 2010, 2012; Pardo-Trujillo et al., 2020; Villagómez & Spikings, 2013). The poor preservation of the magmatic record presents a major limitation for understanding the processes that controlled the evolution of this magmatic arc. As a means to overcome these limitations, we analyzed detrital zircons deposited in a synorogenic basin adjacent to the PECMA and preserved in Bogotá Formation.

We interpret the Paleocene-early Eocene detrital zircon populations recovered from sandstones of the Bogotá Formation to be part of the eroded volcanic and plutonic cover of the PECMA. Previous provenance and stratigraphic analyses of the Bogotá Formation indicate that this sequence formed in a mature fluvial system that drained the paleo-Central Cordillera. This depositional system may have also had a large source area that facilitated sediment mixing (Bayona et al., 2010, 2021; Bustamante et al., 2017). Our results show that samples collected in different stratigraphic positions have progressively younger zircon populations toward the top of the Bogotá Formation, consistent with a scenario in which volcanism is coeval with sedimentation. Despite the induced bias in our analytical strategy (see Section 4.2), samples from similar stratigraphic positions exhibit similar and reproducible zircon age distributions, suggesting a homogenized detrital record of the Paleocene-Eocene magmatism (e.g., samples 860046-1 and 860046-2). This detrital record is older than zircons retrieved from in situ plutonic rocks (Figure 6a) and therefore complements the plutonic record by providing a geochemical fingerprint of the volcanic and plutonic rocks formed during earlier magmatic phases of the PECMA.

6.1. Early Onset of Magmatism Indicates a Short Post-Collisional Magmatic Lull

The plutonic remnants of the PECMA include 62 to 60 Ma plutons and extensive plutonism between 55 and 50 Ma (Figure 1a). In the absence of evidence of earlier magmatism, this fragmentary plutonic record has been interpreted as the result of a magmatic hiatus between 72 and 62 Ma caused by the collision of the Caribbean Plateau (Bayona et al., 2012; Bustamante et al., 2017; Duque-Trujillo, Bustamante, et al., 2019; Jaramillo et al., 2017; Zapata-Villada et al., 2021).

The detrital zircons retrieved from the Bogotá Formation exhibit a longer and more robust record of arc magmatism that spans between 66.0 and 50.9 Ma. The age of this record suggests that following the accretion of the Caribbean Plate at ca. 72 Ma, subduction and magmatism restarted at least by 66 Ma, instead of 62 Ma, as previously interpreted (Bayona et al., 2012; Bustamante et al., 2017; Duque-Trujillo, Bustamante, et al., 2019; Jaramillo et al., 2017; Zapata-Villada et al., 2021). Detrital zircons with ages between 66.0 and 64.0 Ma represent the ∼8% of the Paleocene-Eocene detrital zircon population found in the Bogotá Formation and indicate an earlier onset of post-collisional magmatism. Zircon antecrysts of similar Late Cretaceous-Paleocene age (ca. 66 Ma) have been documented from in situ plutonic rocks of the PECMA, further supporting magmatism that pre-dates 62 Ma. Our finding implies that the magmatic hiatus was shorter (≤6 Ma) than previously proposed (Duque-Trujillo, Bustamante, et al., 2019; Leal-Mejía et al., 2019) and that magmatism was nearly continuous in the transition from a collisional to a subduction setting.

6.2. Geochemistry and Isotopes Reflect Changes in Magma Composition/Magmatic Evolutionary Trends

A clustering analysis based on zircon trace element composition identifies two distinct clusters (Figure 3a): an older cluster that groups 66.0 to 62.0 Ma zircons (Figure 3b), and a younger cluster that includes zircons with ages between 62.0 and 50.9 Ma (Figure 3c). These results show that zircon geochemistry changed significantly after 62.0 Ma and suggest varying conditions in the magmatic processes that controlled the zircon crystallization through time.

6.2.1. Early Stages of Post-Collisional Magmatic Arc Evolution (66.0 to 62.0 Ma)

The 66.0 to 62.0 Ma detrital zircon geochemistry represents the early stages of the arc that followed the Late Cretaceous collision of the Caribbean Plate with the continental margin. This record shows a scenario of limited subduction and magmas that emplaced and differentiated in a thick continental crust (>55 km) that formed during the collision, similar scenarios have been previously suggested (George et al., 2021 and references therein; Leon et al., 2021).

Whole-rock geochemistry of Cretaceous magmatic rocks (100 to 80 Ma) supports the existence of a thin to medium (20–55 km) crust before the collision of the Caribbean Plate with the continental margin (Bustamante et al., 2017; Jaramillo et al., 2017; León et al., 2021). Detrital zircons of Cretaceous age (101.9 to 66.2 Ma) retrieved from the Bogotá Formation agree with this scenario: their low Eu anomalies (Eu/Eu*) are consistent with a medium crust and provide thickness estimates of 44 ± 8 km (Figure S4 in Supporting Information S1. See Section 4). Paleocene detrital zircons from the same sedimentary unit, however, present higher Eu anomalies (Table S1, http://doi.org/10.6084/m9.figshare.19131857), that reflect a thick crust by the early Paleocene and provide crustal thickness estimates between 55 and 80 km (mean value of 72 ± 7.3 km; Figures 6–8). Independent evidence from whole-rock geochemistry of a 65.0 Ma pluton exposed in the Santa Marta Massif reported by Cardona et al. (2011) and Duque-Trujillo et al. (2019) supports this observation. The (La/Yb)n ratio of this pluton provides estimates of a crustal thickness of ca. 50 km (Cardona et al., 2011; Duque-Trujillo, Orozco-Esquivel et al., 2019), and further indicates that the continental crust thickened during the Late Cretaceous. Both the detrital and plutonic record support that a thick crust (>50 km) was in place during the early stages of the PECMA.

The geochemistry of the 66.0 to 62.0 Ma detrital zircon population is suggestive of limited subduction in the early development of the PECMA. The relatively low U content and low U/Yb ratios (Figure 6) are consistent with zircon-forming magmas that are derived from a depleted mantle with a limited presence of fluids. This composition is expected under limited subduction (Barth et al., 2013; Grimes et al., 2015). Even though the 66.0 to 62.0 Ma detrital zircon record overall coincides with a coeval plutonic record, contrasting values of $\varepsilon Hf_{(i)}$ potentially highlight differences in magmatic sources. Whereas detrital zircons have negative $\varepsilon Hf_{(i)}$ values (−4 to −2) (Figure 7f), zircon antecrysts with ages between 66 and 62 Ma found in 55–50 Ma plutonic rocks show positive

$\varepsilon Hf_{(i)}$ values (1.5–5.9) (Bustamante et al., 2017; Cardona et al., 2011). This dissimilarity suggests that between 66 and 62 Ma, magmatic sources were a mixture of juvenile magmas and an old continental crust.

6.2.2. A Continental Margin Dominated by Diverse Magmatic Evolutionary Trends (62 to 50 Ma)

Even though dates from LA-ICP-MS may be inadequate to identify distinct trends in zircon age composition within short time intervals (<10 Ma), the combination of LA-ICP-MS dates and geochemical data with more precise CA-ID-TIMS dates allowed us to identify different compositional pools in zircons with ages between 66.0 and 50.9 Ma. These Younger zircons are characterized by a wider range and differences in mean values of U, U/Yb, Ti, Hf, and crustal thickness when compared to older–66.0 to 62.0 Ma–zircons (Figures 6–8). A wider range in these values suggests the occurrence of both low and highly differentiated and fractionated magmas (Belousova et al., 2002) after 62 Ma. Since Zr/Hf ratios and U values do not exhibit a systematic enrichment and an associated Ti reduction, these variations cannot be explained by the fractionation of a single magma (Grimes et al., 2009; Wang et al., 2010).

The significant increase of the U values and U/Yb ratios after 62 Ma may be indicative of a major input of subducted sediments (Grimes et al., 2015). Ti contents indicate crystallization temperatures between 679°C and 937°C, which also suggests the presence of hot and cold granitic magmas (Miller et al., 2003) (Figures 5d and 7a). Estimates of crustal thickness further indicate that zircons crystallized in both a normal (41 ± 6 km) and a thick (73 ± 9 km) continental crust (Figures 8a and 8b). We interpret that the compositional heterogeneity observed between 62.0 and 50.9 Ma is the result of at least two distinct and unrelated magmatic suites that formed under contrasting crustal architectures.

The *in-situ* plutonic rocks that crystallized between 62 and 50 Ma have geochemical signatures that coincide with those of detrital zircons from the Bogotá Formation (Bustamante et al., 2017; Cardona et al., 2011; Duque-Trujillo, Orozco-Esquivel et al., 2019; Leal-Mejía et al., 2019). Crystallization temperatures calculated from whole-rock geochemistry coincide with the bimodal temperatures inferred from Ti content in detrital zircons (whole-rock geochemistry from Cardona et al., 2011; Leal-Mejia et al., 2019) (Figure 8a). Additionally, whole-rock isotopic data also reveals the presence of low and highly differentiated magma sources (Figures 2 and 7 e.g., Bustamante et al., 2017) (Figure 8b). Finally, these plutonic rocks have (La/Yb)n ratios between 9 and 16, which are characteristic of magmas crystallized in a thick continental crust (>50 km) (Figure 8a).

6.3. Potential Tectonic Controls for Diverse Magmatic Trends in Accretionary Orogens: The Case of the PECMA in the Northern Andes

Major collisional events on accretionary orogens promote extensive deformation and crustal thickening along continental margins (Cawood et al., 2013; van Avendonk et al., 2014). Such changes in the architecture of the crust can modify the composition of the magmas by providing higher pressures for mineral crystallization and facilitating crustal assimilation (Chapman et al., 2015; Chiaradia et al., 2009; S. M. Kay et al., 2014; Profeta et al., 2015). The collision of the Caribbean Plate was one of the major collisional events in the Cretaceous to Cenozoic tectonic evolution history of the Andes and was responsible for the development of high topographic relief (Bayona et al., 2011, 2012; Kennan & Pindell, 2009; Pardo-Trujillo et al., 2020; Villagómez & Spikings, 2013; Zapata et al., 2021). Even though estimates of crustal thickness based on geochemical proxies have noticeable uncertainties (see Section 4.2) and values exceeding 60 km can be abnormally high for Andean-type orogens (S. M. Kay et al., 1991, 2010), we consider that the collision of the Caribbean Plate is a tectonic scenario consistent with the development of a thick continental crust. Sixty-nine percent of the Paleocene-early Eocene detrital zircons analyzed provide crustal thickness estimates between 60 and 90 km. Although the precision of these estimates remains contentious, they agree with a significant (>20 km) crustal thickening during the collision of the Caribbean Plate previously proposed based on geochemical and isotopic data of Late Cretaceous and Paleocene plutons (George et al., 2021; Jaramillo et al., 2017; León et al., 2021).

Detrital zircon geochemistry indicates that after 62 Ma the PECMA was characterized by an increase in the input of subducted sediments, bimodal magmatism, and the coexistence of medium and thick continental crust. The oblique convergence between northwestern South America and the Caribbean Plate margin (Kennan & Pindell, 2009; Montes et al., 2019; Pindell & Kennan, 2009) may account for the magma heterogeneity observed between 62 and 50 Ma. Strike-slip tectonics promoted by oblique convergence was likely to result in coeval transpression and transtension along the continental margin. In this scenario, transtensional settings facilitated

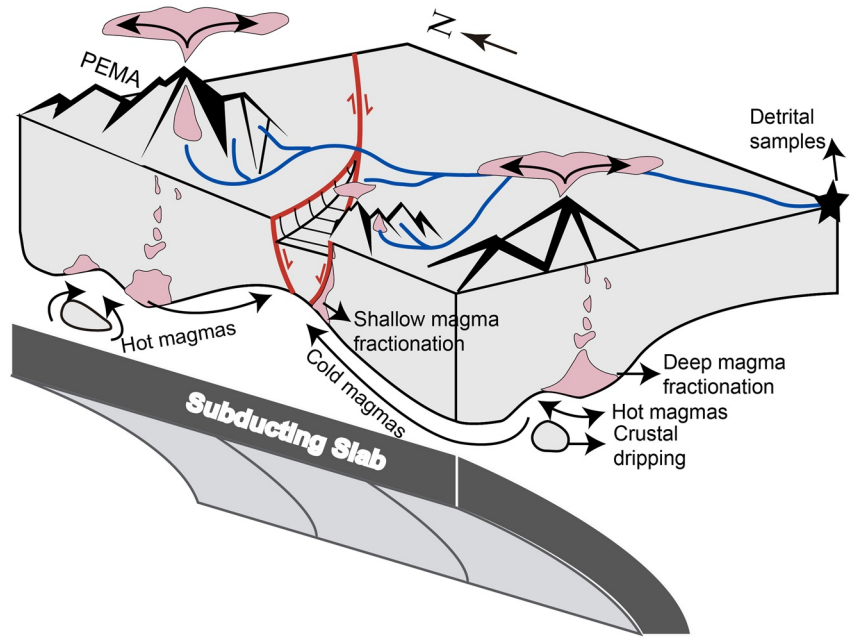

Figure 9. Schematic model of the potential tectonic process that controlled the evolution of the Paleocene-early Eocene continental magmatic arc (PECMA) between 62 and 50 Ma. This figure shows how a magmatic arc developed on a previously thickened continental margin dominated by strike-slip tectonics can be characterized by magmas fractionated at different depths and hot magmas produced by crustal dripping.

the emplacement of juvenile cold and hot magmas under a thin continental crust (McKay et al., 2018; Miller et al., 2003) while transpression maintained the thick continental crust inherited from the collision and promoted high magma differentiation (Figure 9).

Strike-slip tectonics during the Eocene have been previously proposed as a potential driver for the arc shut-off (Bayona et al., 2012; Bustamante et al., 2017; Montes et al., 2019). Additional evidence for strike-slip controls has been observed in the dextrally controlled intrusion of several granitoids crystallized between 58 and 50 Ma (Bustamante et al., 2021; Salazar et al., 2016). Although a significant part of the Paleogene magmatic record was lost by erosion or may be hidden in the crust below, older Jurassic, and Cretaceous arc plutons found in the Central Cordillera have field expressions that are volumetrically larger than the ones from the PECMA (Bustamante et al., 2016; Gómez et al., 2015), and maybe related to lower magmatic productivity between the Paleocene and the early Eocene. This apparent reduction of the magma volumes can be interpreted as evidence of oblique convergence (Sheldrake et al., 2020).

Our data can be partly explained by oblique convergence and strike-slip tectonics. During transtension magmas are formed under a locally thinned continental crust as a consequence of mantle decompression (Kohut et al., 2006; Waldbaum, 1971) and in this extensional setting, water-rich mantle reservoirs produce cold magmas (<800°C) while drier reservoirs generate hotter melts (>800°C) (Holtz & Johannes, 1994; Miller et al., 2003).

The occurrence of hot magmas formed under a thick continental crust inferred from our data (Figures 8a and 8b) is not fully explained by strike-slip tectonics. We suggest that in addition to strike-slip tectonics, lithospheric sinking may have driven mantle upwelling and melting favoring the generation of hot magmas under thick crustal domains (R. W. Kay & Kay, 1993). This process can take place at local and regional scales producing delamination and dripping, respectively, and is associated with the development of a thickened crust that is susceptible to becoming detached (see reviews in Beall et al., 2017; Ducea et al., 2021).

Orogen-scale changes in crustal thickness (up to 40 km) have been documented in several orogens such as the Himalayas, the Central Andes, and Baja California, as a result of major collisional events, crust delamination, and continental extension, respectively (Chen et al., 2020; Priestley et al., 2019; Schmitz et al., 2021). We propose that the combination of a prior thickened crust, local crustal extension, and lithospheric dripping in a scenario of strike-slip tectonics may be responsible for the coexistence of normal and thick continental crust between 62 and 50 Ma in the Northern Andes.

7. Conclusions

1. Detrital zircon age distribution suggests that after the accretion of the Caribbean Plate at 72 Ma, the continental arc magmatism was reestablished under a thickened (>55 km) mixed oceanic-continental crust at least by 66 Ma, earlier than previously proposed (62 Ma).
2. Geochemical signatures of detrital zircons show the existence of both high- and low-pressure fractionation of hot and cold mantle-derived magmas.
3. Oblique tectonics is a plausible mechanism to explain the development of a thinned continental crust that coexisted with a prior thickened crust. Additionally, the presence of zircons crystallized in hot magmas and formed in a thick continental crust may be the record of mantle upwelling related to local crustal sinking (dripping) along the continental margin.
4. Strike-slip deformation combined with local crustal sinking (dripping) tectonics is a plausible mechanism to explain the observed variations in crustal architecture associated with local magmatic differentiation in contrasting crustal architectures between 62 and 55 Ma.

Data Availability Statement

Supplementary methods and tables with the analytical results used for this research are available online (http://doi.org/10.6084/m9.figshare.19131857).

Acknowledgments
The authors thank S. Gómez, N. Chacón, E. Moreno, N. Pérez, A. Tangarife, N. Perdomo for fieldwork support. We acknowledge the support for S. Zapata from the Missouri S&T-STRI Bytnar Postdoctoral Fellowship, and the STRI-Earl S. Tupper postdoctoral fellowship to M. Carvalho. This research was funded by the NSF grant EAR-1829299 (to M. Carvalho and C. Jaramillo). J.S. Jaramillo received funding from the Universidad Nacional de Colombia (grant HERMES 47494). We also acknowledge the colleagues from the EGEO research group at the National University of Colombia for their active discussion. Three anonymous reviewers and the editor Yamirka Rojas-Agramonte are acknowledged for their comments and constructive reviews of the manuscript.

References

Acosta, J. E., & Ulloa, C. E. (1998). Geología de la Plancha 246 Fusagasugá.

Alberts, D., Gehrels, G. E., & Nelson, J. (2021). U-Pb and Hf analyses of detrital zircons from paleozoic and Cretaceous strata on Vancouver Island, British Columbia: Constraints on the paleozoic tectonic evolution of southern Wrangellia. *Lithosphere*, *2021*(1), 1–20. https://doi.org/10.2113/2021/7866944

Barbosa-Espitia, Á. A., Kamenov, G. D., Foster, D. A., Restrepo-Moreno, S. A., & Pardo-Trujillo, A. (2019). Contemporaneous Paleogene arc-magmatism within continental and accreted oceanic arc complexes in the northwestern Andes and Panama. *Lithos*, *348*, 349. https://doi.org/10.1016/j.lithos.2019.105185

Barth, A. P., Wooden, J. L., Jacobson, C. E., & Economos, R. C. (2013). Detrital zircon as a proxy for tracking the magmatic arc system: The California arc example. *Geology*, *41*(2), 223–226. https://doi.org/10.1130/G33619.1

Bayona, G., Baquero, M., Ramírez, C., Tabares, M., Salazar, A. M., Nova, G., et al. (2021). Unraveling the widening of the earliest Andean northern orogen: Maastrichtian to early Eocene intra-basinal deformation in the northern Eastern Cordillera of Colombia. *Basin Research*, *33*(1), 809–845. https://doi.org/10.1111/bre.12496

Bayona, G., Cardona, A., Jaramillo, C., Mora, A., Montes, C., Valencia, V., et al. (2012). Early Paleogene magmatism in the Northern Andes: Insights on the effects of Oceanic Plateau-continent convergence. *Earth and Planetary Science Letters*, *331–332*, 97–111. https://doi.org/10.1016/j.epsl.2012.03.015

Bayona, G., Montenegro, O., Cardona, A., Jaramillo, C., & Lamus, F. (2010). Estratigrafía, procedencia, subsidencia y exhumación de las unidades paleógenas en el Sinclinal de Usme, sur de la zona axial de la Cordillera Oriental. *Geología Colombiana*, *35*(0), 5–35.

Bayona, G., Montes, C., Cardona, A., Jaramillo, C., Ojeda, G., Valencia, V., & Ayala-Calvo, C. (2011). Intraplate subsidence and basin filling adjacent to an oceanic arc-continent collision: A case from the southern Caribbean-South America plate margin. *Basin Research*, *23*(4), 403–422. https://doi.org/10.1111/j.1365-2117.2010.00495.x

Beall, A. P., Moresi, L., & Stern, T. (2017). Dripping or delamination? A range of mechanisms for removing the lower crust or lithosphere. *Geophysical Journal International*, *210*(2), 671–692. https://doi.org/10.1093/gji/ggx202

Belousova, E. A., Griffin, W. L., O'Reilly, S. Y., & Fisher, N. I. (2002). Igneous zircon: Trace element composition as an indicator of source rock type. *Contributions to Mineralogy and Petrology*, *143*(5), 602–622. https://doi.org/10.1007/s00410-002-0364-7

Black, L. P., Kamo, S. L., Allen, C. M., Davis, D. W., Aleinikoff, J. N., Valley, J. W., et al. (2004). Improved 206Pb/238U microprobe geochronology by the monitoring of a trace-element-related matrix effect; SHRIMP, ID-TIMS, ELA-ICP-MS and oxygen isotope documentation for a series of zircon standards. *Chemical Geology*, *205*(1–2), 115–140. https://doi.org/10.1016/j.chemgeo.2004.01.003

Brown, D., & Ryan, P. D. (2011). Arc-continent collision. *Frontiers of Earth Science*, *4*, 477–493. https://doi.org/10.1007/978-3-540-88558-0

Bustamante, C., Archanjo, C. J., Cardona, A., & Restrepo, M. (2021). Magnetic fabric of the Parashi stock and related dyke swarm, Alta Guajira (Colombia): The Caribbean-South American plates oblique convergence. *Andean Geology*, *48*(2), 219–236. https://doi.org/10.5027/andgeov48n2-3332

Bustamante, C., Archanjo, C. J., Cardona, A., & Vervoort, J. D. (2016). Late Jurassic to early Cretaceous plutonism in the Colombian Andes: A record of long-term arc maturity. *Bulletin of the Geological Society of America*, *128*(11–12), 1762–1779. https://doi.org/10.1130/B31307.1

Bustamante, C., Cardona, A., Archanjo, C. J., Bayona, G., Lara, M., & Valencia, V. (2017). Geochemistry and isotopic signatures of Paleogene plutonic and detrital rocks of the Northern Andes of Colombia: A record of post-collisional arc magmatism. *Lithos*, *277*, 199–209. https://doi.org/10.1016/j.lithos.2016.11.025

Caballero, V. M., Rodríguez, G., Naranjo, J. F., Mora, A., & De La Parra, F. (2020). From Facies analysis, Stratigraphic surfaces, and depositional sequences to stratigraphic traps in the Eocene—Oligocene record of the Southern Llanos Basin and Northern Magdalena basin. In *The geology of Colombia* (pp. 283–330).

Cardona, A., León, S., Jaramillo, J. S., Montes, C., Valencia, V., Vanegas, J., et al. (2018). The Paleogene arcs of the northern Andes of Colombia and Panama: Insights on plate kinematic implications from new and existing geochemical, geochronological and isotopic data. *Tectonophysics*, *749*, 88–103. https://doi.org/10.1016/j.tecto.2018.10.032

Cardona, A., Valencia, V. A., Bayona, G., Duque, J., Ducea, M., Gehrels, G., et al. (2011). Early-subduction-related orogeny in the Northern Andes: Turonian to Eocene magmatic and provenance record in the Santa Marta Massif and Rancheria basin, northern Colombia. *Terra Nova*, *23*(1), 26–34. https://doi.org/10.1111/j.1365-3121.2010.00979.x

Cavosie, A. J., Valley, J. W., & Wilde, S. A. (2006). Correlated microanalysis of zircon: Trace element, $\delta^{18}O$, and U-Th-Pb isotopic constraints on the igneous origin of complex >3900 Ma detrital grains. *Geochimica et Cosmochimica Acta*, *70*(22), 5601–5616. https://doi.org/10.1016/j.gca.2006.08.011

Cavosie, A. J., Valley, J. W., Wilde, S. A., & E.i.m.f. (2005). Magmatic $\delta^{18}O$ in 4400–3900 Ma detrital zircons: A record of the alteration and recycling of crust in the early Archean. *Earth and Planetary Science Letters*, *235*(3–4), 663–681. https://doi.org/10.1016/j.epsl.2005.04.028

Cawood, P. A., Hawkesworth, C. J., & Dhuime, B. (2013). The continental record and the generation of continental crust. *Bulletin of the Geological Society of America*, *125*(1–2), 14–32. https://doi.org/10.1130/B30722.1

Chapman, J. B., Ducea, M. N., DeCelles, P. G., & Profeta, L. (2015). Tracking changes in crustal thickness during orogenic evolution with Sr/Y: An example from the North American Cordillera. *Geology*, *43*(10), 919–922. https://doi.org/10.1130/G36996.1

Chen, J., Kufner, S. K., Yuan, X., Heit, B., Wu, H., Yang, D., et al. (2020). Lithospheric delamination beneath the southern Puna plateau resolved by local earthquake tomography. *Journal of Geophysical Research: Solid Earth*, *125*(10), 1–17. https://doi.org/10.1029/2019JB019040

Chiaradia, M., Müntener, O., Beate, B., & Fontignie, D. (2009). Adakite-like volcanism of Ecuador: Lower crust magmatic evolution and recycling. *Contributions to Mineralogy and Petrology*, *158*(5), 563–588. https://doi.org/10.1007/s00410-009-0397-2

Cilliers, C. D., Tucker, R. T., Crowley, J. L., & Zanno, L. E. (2021). Age constraint for the Moreno hill formation (Zuni basin) by CA-TIMS and LA-ICP-MS detrital zircon geochronology. *PeerJ*, *9*, 1–39. https://doi.org/10.7717/peerj.10948

Claiborne, L. L., Miller, C. F., Walker, B. A., Wooden, J. L., Mazdab, F. K., & Bea, F. (2006). Tracking magmatic processes through Zr/Hf ratios in rocks and Hf and Ti zoning in zircons: An example from the Spirit Mountain batholith, Nevada. *Mineralogical Magazine*, *70*(5), 517–543. https://doi.org/10.1180/0026461067050348

Claiborne, L. L., Miller, C. F., & Wooden, J. L. (2010). Trace element composition of igneous zircon: A thermal and compositional record of the accumulation and evolution of a large silicic batholith, Spirit Mountain, Nevada. *Contributions to Mineralogy and Petrology*, *160*(4), 511–531. https://doi.org/10.1007/s00410-010-0491-5

Condon, D. J., Schoene, B., McLean, N. M., Bowring, S. A., & Parrish, R. (2015). Metrology and traceability of U-Pb isotope dilution geochronology (EARTHTIME Tracer Calibration Part I). *Geochimica et Cosmochimica Acta*, *164*, 464–480.

Corfu, F., Hanchar, J. M., Hoskin, P. W. O., & Kinny, P. (2003). Atlas of zircon textures. *Zircon*, *53*(1), 469–500.

Crowley, J. L., Schoene, B., & Bowring, S. A. (2007). U-Pb dating of zircon in the Bishop Tuff at the millennial scale. *Geology*, *35*(12), 1123–1126. https://doi.org/10.1130/G24017A.1

Draut, A. E., & Clift, P. D. (2001). Geochemical evolution of arc magmatism during arc-continent collision, South Mayo, Ireland. *Geology*, *29*(6), 543–546. https://doi.org/10.1130/0091-7613(2001)029<0543:GEOAMD>2.0.CO;2

Ducea, M. N., Chapman, A. D., Bowman, E., & Triantafyllou, A. (2021). Arclogites and their role in continental evolution; part 1: Background, locations, petrography, geochemistry, chronology and thermobarometry. *Earth-Science Reviews*, *214*, 103375. https://doi.org/10.1016/j.earscirev.2020.103375

Ducea, M. N., Saleeby, J. B., & Bergantz, G. (2015). The architecture, chemistry, and evolution of continental magmatic arcs. *Annual Review of Earth and Planetary Sciences*, *43*, 299–331. https://doi.org/10.1146/annurev-earth-060614-105049

Duque-Trujillo, J. F., Bustamante, C., Solari, L., Gómez-Mafla, Á., Toro-Villegas, G., Hoyos, S., & Sato, A. M. (2019). Reviewing the Antioquia batholith and satellite bodies: A record of late Cretaceous to Eocene syn-to post-collisional arc magmatism in the Central Cordillera of Colombia. *Andean Geology*, *46*(1), 82–101. https://doi.org/10.5027/andgeoV46n1-3124

Duque-Trujillo, J. F., Orozco-Esquivel, T., Sánchez, C. J., & Cárdenas-Rozo, A. L. (2019). Paleogene magmatism of the Maracaibo Block and its tectonic significance. *Geology and Tectonics of Northwestern South America, Frontiers in Earth Sciences*, 551–601. https://doi.org/10.1007/978-3-319-76132-9_7

Ferry, J. M., & Watson, E. B. (2007). New thermodynamic models and revised calibrations for the Ti-in-zircon and Zr-in-rutile thermometers. *Contributions to Mineralogy and Petrology*, *154*(4), 429–437. https://doi.org/10.1007/s00410-007-0201-0

Gaschnig, R. M., Vervoort, J. D., Tikoff, B., & Lewis, R. S. (2017). Construction and preservation of batholiths in the northern U.S. Cordillera. *Lithosphere*, *9*(2), 315–324. https://doi.org/10.1130/L497.1

Gehrels, G. (2014). Detrital zircon U-Pb geochronology applied to tectonics. *Annual Review of Earth and Planetary Sciences*, *42*(1), 127–149. https://doi.org/10.1146/annurev-earth-050212-124012

Gehrels, G., Valencia, V. A., & Ruiz, J. (2008). Enhanced precision, accuracy, efficiency, and spatial resolution of U-Pb ages by laser ablation-multicollector-inductively coupled plasma-mass spectrometry. *Geochemistry, Geophysics, Geosystems*, *9*(3), 1–13. https://doi.org/10.1029/2007GC001805

George, S. W. M., Horton, B. K., Vallejo, C., Jackson, L. J., & Gutierrez, E. G. (2021). Did accretion of the Caribbean oceanic plateau drive rapid crustal thickening in the Northern Andes? *Geology*, *49*(8), 936–940. https://doi.org/10.1130/g48509.1

Gerstenberger, H., & Haase, G. (1997). A highly effective emitter substance for mass spectrometric Pb isotope ratio determinations. *Chemical Geology*, *136*(3–4), 309–312. https://doi.org/10.1016/s0009-2541(96)00033-2

Gerya, T. V., & Meilick, F. I. (2011). Geodynamic regimes of subduction under an active margin: Effects of rheological weakening by fluids and melts. *Journal of Metamorphic Geology*, *29*(1), 7–31. https://doi.org/10.1111/j.1525-1314.2010.00904.x

Glazner, A. F., Coleman, D. S., & Mills, R. D. (2015). The Volcanic-Plutonic Connection. https://doi.org/10.1007/11157

Gómez, J., Nivia, Á., Montes, N. E., Almanza, M. F., Alcárcel, F. A., & Madrid, C. A. (2015). Compilando la geología de Colombia: Una visión a 2015. Bogotá. Servicio Geológico Colombiano, Publicaciones Geológicas Especiales (Vol. *33*).

González, P. D., Sato, A. M., Naipauer, M., Varela, R., Basei, M., Sato, K., et al. (2018). Patagonia-Antarctica Early Paleozoic conjugate margins: Cambrian synsedimentary silicic magmatism, U-Pb dating of K-bentonites, and related volcanogenic rocks. *Gondwana Research*, *63*, 186–225. https://doi.org/10.1016/j.gr.2018.05.015

Grimes, C. B., John, B. E., Cheadle, M. J., Mazdab, F. K., Wooden, J. L., Swapp, S., & Schwartz, J. J. (2009). On the occurrence, trace element geochemistry, and crystallization history of zircon from in situ ocean lithosphere. *Contributions to Mineralogy and Petrology*, *158*(6), 757–783. https://doi.org/10.1007/s00410-009-0409-2

Grimes, C. B., Wooden, J. L., Cheadle, M. J., & John, B. E. (2015). "Fingerprinting" tectono-magmatic provenance using trace elements in igneous zircon. *Contributions to Mineralogy and Petrology*, *170*(5–6), 1–26. https://doi.org/10.1007/s00410-015-1199-3

Herriott, T. M., Crowley, J. L., Schmitz, M. D., Wartes, M. A., & Gillis, R. J. (2019). Exploring the law of detrital zircon: LA-ICP-MS and CA-TIMS geochronology of Jurassic forearc strata, Cook inlet, Alaska, USA. *Geology*, *47*(11), 1044–1048. https://doi.org/10.1130/G46312.1

Hiess, J., Condon, D. J., McLean, N., & Noble, S. R. (2012). $^{238}U/^{235}U$ systematics in terrestrial uranium-bearing minerals. *Science*, *335*(6076), 1610–1614. https://doi.org/10.1126/science.1215507

Holder, R. M., Yakymchuk, C., & Viete, D. R. (2020). Accessory mineral Eu anomalies in Suprasolidus rocks: Beyond Feldspar. *Geochemistry, Geophysics, Geosystems*, *21*(8), 1–16. https://doi.org/10.1029/2020GC009052

Holtz, F., & Johannes, W. (1994). Maximum and minimum water contents of granitic melts: Implications for chemical and physical properties of ascending magmas. *Lithos*, *32*(1–2), 149–159. https://doi.org/10.1016/0024-4937(94)90027-2

Horton, B. K. (2018). Sedimentary record of Andean mountain building. *Earth-Science Reviews*, *178*, 279–309. https://doi.org/10.1016/j.earscirev.2017.11.025

Horton, B. K., Anderson, V. J., Caballero, V., Saylor, J. E., Nie, J., Parra, M., & Mora, A. (2015). Application of detrital zircon U-Pb geochronology to surface and subsurface correlations of provenance, paleodrainage, and tectonics of the Middle Magdalena Valley Basin of Colombia. *Geosphere*, *11*(6), 1790–1811. https://doi.org/10.1130/GES01251.1

Horton, B. K., Saylor, J. E., Nie, J., Mora, A., Parra, M., Reyes-Harker, A., & Stockli, D. F. (2010). Linking sedimentation in the northern Andes to basement configuration, Mesozoic extension, and Cenozoic shortening: Evidence from detrital zircon U-Pb ages, Eastern Cordillera, Colombia. *Bulletin of the Geological Society of America*, *122*(9–10), 1423–1442. https://doi.org/10.1130/B30118.1

Iizuka, T., Yamaguchi, T., Itano, K., Hibiya, Y., & Suzuki, K. (2017). What Hf isotopes in zircon tell us about crust-mantle evolution. *Lithos*, *274–275*, 304–327. https://doi.org/10.1016/j.lithos.2017.01.006

Jaffey, A. H., Flynn, K. F., Glendenin, L. E., Bentley, W. C., & Essling, A. M. (1971). Precision measurements of half-lives and specific activities of 235U and 238U. *Physical Review C*, *4*, 1889–1906.

Jaramillo, C., & Cárdenas, A. (2013). Global warming and neotropical rainforests: A historical perspective. *Annual Review of Earth and Planetary Sciences*, *41*(1), 741–766. https://doi.org/10.1146/annurev-earth-042711-105403

Jaramillo, J. S., Cardona, A., León, S., Valencia, V., & Vinasco, C. (2017). Geochemistry and geochronology from Cretaceous magmatic and sedimentary rocks at 6°35′N, Western flank of the Central cordillera (Colombian Andes): Magmatic record of arc growth and collision. *Journal of South American Earth Sciences*, *76*, 460–481. https://doi.org/10.1016/j.jsames.2017.04.012

Juggins, S. (2020). rioja: Analysis of quaternary science data, R package version (0.9-26). Retrieved from https://cran.r-project.org/package=rioja

Kaoungku, N., Suksut, K., Chanklan, R., Kerdprasop, K., & Kerdprasop, N. (2018). The silhouette width criterion for clustering and association mining to select image features. *International Journal of Machine Learning and Computing*, *8*(1), 69–73. https://doi.org/10.18178/ijmlc.2018.8.1.665

Kay, R. W., & Kay, S. M. (1993). Delamination and delamination. *Tectono*, *219*, 177–189.

Kay, S. M., Coira, B. L., Caffe, P. J., & Chen, C. H. (2010). Regional chemical diversity, crustal and mantle sources and evolution of central Andean Puna plateau ignimbrites. *Journal of Volcanology and Geothermal Research*, *198*(1–2), 81–111. https://doi.org/10.1016/j.jvolgeores.2010.08.013

Kay, S. M., Mpodozis, C., & Gardeweg, M. (2014). Magma sources and tectonic setting of Central Andean andesites (25.5–288S) related to crustal thickening, forearc subduction erosion and delamination. *Geological Society—Special Publications*, *385*(1), 303–334. https://doi.org/10.1144/SP385.11

Kay, S. M., Mpodozis, C., Ramos, V. A., & Munizaga, F. (1991). Magma source variations for mid-late Tertiary magmatic rocks associated with a shallowing subduction zone and a thickening crust in the central Andes (28 to 33°S). *Geological Society of America Special Publication*, *265*, 113–137.

Kennan, L., & Pindell, J. L. (2009). Dextral shear, terrane accretion and basin formation in the Northern Andes: Best explained by interaction with a Pacific-derived Caribbean plate? *Geological Society—Special Publications*, *328*, 487–531. https://doi.org/10.1144/SP328.20

Kennedy, A. K., Wotzlaw, J. F., Schaltegger, U., Crowley, J. L., & Schmitz, M. (2014). Eocene zircon reference material for microanalysis of U-Th-Pb isotopes and trace elements. *The Canadian Mineralogist*, *52*(3), 409–421. https://doi.org/10.3749/canmin.52.3.409

Kerr, A. C., Marriner, G. F., Tarney, J., Nivia, A., Saunders, A. D., Thirlwall, M. F., & Sinton, C. W. (1997). Cretaceous basaltic terranes in Western Colombia: Elemental, chronological and Sr-Nd isotopic constraints on petrogenesis. *Journal of Petrology*, *38*(6), 677–702. https://doi.org/10.1093/petroj/38.6.677

Kirkland, C. L., Smithies, R. H., Taylor, R. J. M., Evans, N., & McDonald, B. (2015). Zircon Th/U ratios in magmatic environs. *Lithos*, *212–215*, 397–414. https://doi.org/10.1016/j.lithos.2014.11.021

Kohut, E. J., Stern, R. J., Kent, A. J. R., Nielsen, R. L., Bloomer, S. H., & Leybourne, M. (2006). Evidence for adiabatic decompression melting in the Southern Mariana Arc from high-Mg lavas and melt inclusions. *Contributions to Mineralogy and Petrology*, *152*(2), 201–221. https://doi.org/10.1007/s00410-006-0102-7

Krogh, T. E. (1973). A low contamination method for hydrothermal decomposition of zircon and extraction of U and Pb for isotopic age determination. *Geochimica et Cosmochimica Acta*, *37*(3), 485–494. https://doi.org/10.1016/0016-7037(73)90213-5

Leal-Mejía, H. (2011). Phanerozoic gold metallogeny in the Colombian Andes: A tectono-magmatic approach.

Leal-Mejía, H., Shaw, R. P., & i Draper, J. C. M. (2019). Spatial-temporal migration of granitoid magmatism and the Phanerozoic tectono-magmatic evolution of the Colombian Andes. In *Geology and tectonics of northwestern South America* (pp. 253–410). Springer.

León, S., Cardona, A., Parra, M., Sobel, E. R., Jaramillo, J. S., Glodny, J., et al. (2018). Transition from collisional to Subduction-related regimes: An example from Neogene Panama-Nazca-South America interactions. *Tectonics*, *37*(1), 119–139. https://doi.org/10.1002/2017TC004785

León, S., Monsalve, G., & Bustamante, C. (2021). How Much did the Colombian Andes rise by the collision of the Caribbean Oceanic Plateau? *Geophysical Research Letters*, *48*(7), 1–11. https://doi.org/10.1029/2021GL093362

Levene, H. (1960). Robust tests for equality of variances. In I. Olkin (Ed.), *Contributions to probability and statistics* (pp. 278–292). Stanford University Press. Chapter 25.

Ludwig, K. R. (2003). *User's manual for Isoplot 3.00* (p. 70). Berkeley Geochronology Center.

Malusà, M. G., Villa, I. M., Vezzoli, G., & Garzanti, E. (2011). Detrital geochronology of unroofing magmatic complexes and the slow erosion of Oligocene volcanoes in the Alps. *Earth and Planetary Science Letters*, *301*(1–2), 324–336. https://doi.org/10.1016/j.epsl.2010.11.019

Mann, H. B., & Whitney, D. R. (1947). On a test of whether one of two random variables is stochastically larger than the other. *The Annals of Mathematical Statistics*, *18*(1), 50–60. https://doi.org/10.1214/aoms/1177730491

Mattinson, J. M. (2005). Zircon U-Pb chemical abrasion ("CA-TIMS") method: Combined annealing and multi-step partial dissolution analysis for improved precision and accuracy of zircon ages. *Chemical Geology*, *220*(1–2), 47–66. https://doi.org/10.1016/j.chemgeo.2005.03.011

McDonough, W. F., & Sun, S.-S. (1995). The composition of the Earth. *Chemical Geology*, *120*(3–4), 223–253. https://doi.org/10.1016/0009-2541(94)00140-4

McKay, M. P., Jackson, W. T., & Hessler, A. M. (2018). Tectonic stress regime recorded by zircon Th/U. *Gondwana Research*, *57*, 1–9. https://doi.org/10.1016/j.gr.2018.01.004

McKenzie, N. R., Smye, A. J., Hegde, V. S., & Stockli, D. F. (2018). Continental growth histories revealed by detrital zircon trace elements: A case study from India. *Geology*, *46*(3), 275–278. https://doi.org/10.1130/G39973.1

Miller, C. F., McDowell, S. M., & Mapes, R. W. (2003). Hot and cold granites: Implications of zircon saturation temperatures and preservation of inheritance. *Geology*, *31*(6), 529–532. https://doi.org/10.1130/0091-7613(2003)031<0529:HACGIO>2.0.CO;2

Montes, C., Cardona, A., Jaramillo, C., Pardo, A., Silva, J. C., Valencia, V., et al. (2015). Middle Miocene closure of the Central American Seaway. *Science*, *348*(6231), 226–229. https://doi.org/10.1126/science.aaa2815

Montes, C., Cardona, A., McFadden, R., Morón, S. E., Silva, C. A., Restrepo-Moreno, S., et al. (2012). Evidence for middle Eocene and younger land emergence in central Panama: Implications for Isthmus closure. *Bulletin of the Geological Society of America*, *124*(5–6), 780–799. https://doi.org/10.1130/B30528.1

Montes, C., Guzman, G., Bayona, G., Cardona, A., Valencia, V., & Jaramillo, C. (2010). Clockwise rotation of the Santa Marta massif and simultaneous Paleogene to Neogene deformation of the Plato-San Jorge and Cesar-Ranchería basins. *Journal of South American Earth Sciences*, *29*(4), 832–848. https://doi.org/10.1016/j.jsames.2009.07.010

Montes, C., Rodriguez-Corcho, A. F., Bayona, G., Hoyos, N., Zapata, S., & Cardona, A. (2019). Continental margin response to multiple arc-continent collisions: The Northern Andes-Caribbean margin. *Earth-Science Reviews*, *198*, 102903. https://doi.org/10.1016/j.earscirev.2019.102903

Morón, S., Fox, D. L., Feinberg, J. M., Jaramillo, C., Bayona, G., Montes, C., & Bloch, J. I. (2013). Climate change during the Early Paleogene in the Bogotá Basin (Colombia) inferred from paleosol carbon isotope stratigraphy, major oxides, and environmental magnetism. *Palaeogeography, Palaeoclimatology, Palaeoecology*, *388*, 115–127. https://doi.org/10.1016/j.palaeo.2013.08.010

Morton, A. C., & Hallsworth, C. (2007). Stability of detrital heavy minerals during burial diagenesis. *Developments in Sedimentology*, *58*, 215–245.

Ordoñez, O., Pimentel, M., Armstrong, R., Gioias, S., & Junges, S. (2001). U-Pb SHRIMP and Rb-Sr ages of the SONSÓN BATHOLITH. *Symposium A Quarterly Journal in Modern Foreign Literatures*.

Pardo-Trujillo, A., Cardona, A., Giraldo, A. S., León, S., Vallejo, D. F., Trejos-Tamayo, R., et al. (2020). Sedimentary record of the Cretaceous–Paleocene arc–continent collision in the northwestern Colombian Andes: Insights from stratigraphic and provenance constraints. *Sedimentary Geology*, *401*, 105627. https://doi.org/10.1016/j.sedgeo.2020.105627

Parra, M., Echeverri, S., Patiño, A. M., Ramírez, J. C., Mora, A., Sobel, E. R., et al. (2020). Cenozoic evolution of the Sierra Nevada de Santa Marta, Colombia. *The Geology of Colombia Paleogene–Neogene*, *3*, 185–213. https://doi.org/10.32685/pub.esp.37.2019.07

Paterson, B. A., & Stephens, W. E. (1992). Kinetically induced compositional zoning in titanite: Implications for accessory-phase/melt partitioning of trace elements. *Contributions to Mineralogy and Petrology*, *109*(3), 373–385. https://doi.org/10.1007/BF00283325

Paterson, S. R., & Ducea, M. N. (2015). Arc magmatic tempos: Gathering the evidence. *Elements*, *11*(2), 91–98. https://doi.org/10.2113/gselements.11.2.91

Pindell, J. L., & Kennan, L. (2009). Tectonic evolution of the Gulf of Mexico, Caribbean and northern South America in the mantle reference frame: An update. *Geological Society—Special Publications*, *328*(1982), 1–55. https://doi.org/10.1144/SP328.1

Priestley, K., Ho, T., & Mitra, S. (2019). The crustal structure of the Himalaya: A synthesis. *Geological Society, London, Special Publications*, *483*(1), 483–516. https://doi.org/10.1144/sp483-2018-127

Profeta, L., Ducea, M. N., Chapman, J. B., Paterson, S. R., Gonzales, S. M. H., Kirsch, M., et al. (2015). Quantifying crustal thickness over time in magmatic arcs. *Scientific Reports*, *5*, 1–7. https://doi.org/10.1038/srep17786

Restrepo, J. J., & Toussaint, J. F. (1988). Terranes and continental accretion in the Colombian Andes. *Episodes*, *11*(3), 189–193. https://doi.org/10.18814/epiiugs/1988/v11i3/006

Rodríguez-Alonso, M. D., Peinado, M., López-Plaza, M., Franco, P., Carnicero, A., & Gonzalo, J. C. (2004). Neoproterozoic-Cambrian synsedimentary magmatism in the Central Iberian Zone (Spain): Geology, petrology and geodynamic significance. *International Journal of Earth Sciences*, *93*(5), 897–920. https://doi.org/10.1007/s00531-004-0425-4

Rubatto, D. (2017). Zircon: The metamorphic mineral. *Reviews in Mineralogy and Geochemistry*, *83*(1), 261–295. https://doi.org/10.2138/rmg.2017.83.09

Rueda-Gutiérrez, J. B. (2019). Contributions to the magmatism knowledge of the Central Cordillera of Colombia in its eastern flank: Geothermal area of San diego, Samaná, Caldas. *Boletin de Geologia*, *41*(2), 45–70. https://doi.org/10.18273/revbol.v41n2-2019003

Salazar, C. A., Bustamante, C., & Archanjo, C. J. (2016). Magnetic fabric (AMS, AAR) of the Santa Marta batholith (northern Colombia) and the shear deformation along the Caribbean Plate margin. *Journal of South American Earth Sciences*, *70*, 55–68. https://doi.org/10.1016/j.jsames.2016.04.011

Schaltegger, U., Schmitt, A. K., & Horstwood, M. S. A. (2015). U-Th-Pb zircon geochronology by ID-TIMS, SIMS, and laser ablation ICP-MS: Recipes, interpretations, and opportunities. *Chemical Geology*, *402*, 89–110. https://doi.org/10.1016/j.chemgeo.2015.02.028

Schmitz, M., Ramírez, K., Mazuera, F., Ávila, J., Yegres, L., Bezada, M., & Levander, A. (2021). Moho depth map of northern Venezuela based on wide-angle seismic studies. *Journal of South American Earth Sciences*, *107*, 103088. https://doi.org/10.1016/j.jsames.2020.103088

Schmitz, M. D., & Schoene, B. (2007). Derivation of isotope ratios, errors and error correlations for U-Pb geochronology using 205Pb-235U-(233U)-spiked isotope dilution thermal ionization mass spectrometric data. *Geochemistry, Geophysics, Geosystems*, *8*(8), Q08006. https://doi.org/10.1029/2006GC001492

Schwartz, T. M., Surpless, K. D., Colgan, J. P., Johnstone, S. A., & Holm-Denoma, C. S. (2021). Detrital zircon record of magmatism and sediment dispersal across the North American Cordilleran arc system (28–48°N). *Earth-Science Reviews*, *220*, 103734. https://doi.org/10.1016/j.earscirev.2021.103734

Sheldrake, T., Caricchi, L., & Scutari, M. (2020). Tectonic controls on global variations of large-magnitude explosive eruptions in volcanic arcs. *Frontiers of Earth Science*, *8*, 1–14. https://doi.org/10.3389/feart.2020.00127

Sláma, J., Košler, J., Condon, D. J., Crowley, J. L., Gerdes, A., Hanchar, J. M., et al. (2008). Plešovice zircon—A new natural reference material for U–Pb and Hf isotopic microanalysis. *Chemical Geology*, *249*(1–2), 1–35. https://doi.org/10.1016/j.chemgeo.2007.11.005

Sundell, K. E., Laskowski, A. K., Kapp, P. A., Ducea, M. N., & Chapman, J. B. (2021). Jurassic to Neogene quantitative crustal thickness estimates in southern Tibet. *Geological Society of America Today*, *31*(6), 4–10. https://doi.org/10.1130/gsatg461a.1

Syracuse, E. M., & Abers, G. A. (2006). Global compilation of variations in slab depth beneath arc volcanoes and implications. *Geochemistry, Geophysics, Geosystems*, *7*(5), Q05017. https://doi.org/10.1029/2005GC001045

Tang, M., Erdman, M., Eldridge, G., & Lee, C.-T. A. (2018). The redox "filter" beneath magmatic orogens and the formation of continental crust. *Science Advances*, *4*(5), eaar4444. https://doi.org/10.1126/sciadv.aar4444

Tang, M., Ji, W. Q., Chu, X., Wu, A., & Chen, C. (2021). Reconstructing crustal thickness evolution from europium anomalies in detrital zircons. *Geology*, *49*(1), 76–80. https://doi.org/10.1130/G47745.1

Tang, M., Lee, C.-T. A., Costin, G., & Höfer, H. E. (2019). Recycling reduced iron at the base of magmatic orogens. *Earth and Planetary Science Letters*, *528*, 115827. https://doi.org/10.1016/j.epsl.2019.115827

van Avendonk, H. J., Kuo-Chen, H., Mcintosh, K. D., Lavier, L. L., Okaya, D. A., Wu, F. T., et al. (2014). Deep crustal structure of an arc-continent collision: Constraints from seismic traveltimes in central Taiwan and the Philippine Sea. *Journal of Geophysical Research: Solid Earth*, *119*(11), 8397–8416. https://doi.org/10.1002/2014JB011327.Received

Vermeesch, P. (2018). IsoplotR: A free and open toolbox for geochronology. *Geoscience Frontiers*, *9*(5), 1479–1493. https://doi.org/10.1016/j.gsf.2018.04.001

Vermeesch, P. (2021). Maximum depositional age estimation revisited. *Geoscience Frontiers*, *12*(2), 843–850. https://doi.org/10.1016/j.gsf.2020.08.008

Vervoort, J. D., Patehett, P. J., Söderlund, U., & Baker, M. (2004). Isotopie composition of Yb and the determination of Lu concentrations and Lu/Hf ratios by isotope dilution using MC-ICPMS. *Geochemistry, Geophysics, Geosystems*, *5*(11),Q11002. https://doi.org/10.1029/2004GC000721

Villagómez, D., & Spikings, R. (2013). Thermochronology and tectonics of the Central and Western Cordilleras of Colombia: Early Cretaceous-tertiary evolution of the Northern Andes. *Lithos*, *160–161*(1), 228–249. https://doi.org/10.1016/j.lithos.2012.12.008

Villagómez, D., Spikings, R., Magna, T., Kammer, A., Winkler, W., & Beltrán, A. (2011). Geochronology, geochemistry and tectonic evolution of the Western and Central cordilleras of Colombia. *Lithos*, *125*(3–4), 875–896. https://doi.org/10.1016/j.lithos.2011.05.003

Waldbaum, D. R. (1971). Temperature changes associated with adiabatic decompression in geological processes. *Nature*, *232*(5312), 545–547. https://doi.org/10.1038/232545a0

Wang, X., Griffin, W. L., & Chen, J. (2010). Hf contents and Zr/Hf ratios in granitic zircons. *Geochemical Journal*, *44*(1), 65–72. https://doi.org/10.2343/geochemj.1.0043

Weber, M., Cardona, A., Valencia, V., García-Casco, A., Tobón, M., & Zapata, S. (2010). U/Pb detrital zircon provenance from late cretaceous metamorphic units of the Guajira Peninsula, Colombia: Tectonic implications on the collision between the Caribbean arc and the South American margin. *Journal of South American Earth Sciences*, *29*(4), 805–816. https://doi.org/10.1016/j.jsames.2009.10.004

Yang, J., Cawood, P. A., Du, Y., Huang, H., Huang, H., & Tao, P. (2012). Large Igneous Province and magmatic arc sourced Permian-Triassic volcanogenic sediments in China. *Sedimentary Geology*, *261–262*, 120–131. https://doi.org/10.1016/j.sedgeo.2012.03.018

Zapata, S., Zapata-Henao, M., Cardona, A., Jaramillo, C., Silvestro, D., & Oboh-Ikuenobe, F. (2021). Long-term topographic growth and decay constrained by 3D thermo-kinematic modeling: Tectonic evolution of the Antioquia Altiplano, Northern Andes. *Global and Planetary Change*, *203*, 103553. https://doi.org/10.1016/j.gloplacha.2021.103553

Zapata-García, G., & Rodríguez-García, G. (2020). New contributions to knowledge about the Chocó-Panamá arc in Colombia, including a new segment south of Colombia. *The Geology of Colombia*, *3*, 417–450.

Zapata-Villada, J. P., Cardona, A., Serna, S., & Rodríguez, G. (2021). Late Cretaceous to Paleocene magmatic record of the transition between collision and subduction in the western and central Cordillera of northern Colombia. *Journal of South American Earth Sciences*, *112*(P1), 103557. https://doi.org/10.1016/j.jsames.2021.103557

Zimmerer, M. J., & McIntosh, W. C. (2012). The geochronology of volcanic and plutonic rocks at the Questa caldera: Constraints on the origin of caldera-related silicic magmas. *Bulletin of the Geological Society of America*, *124*(7–8), 1394–1408. https://doi.org/10.1130/B30544.1